

# Crystalor: Recoverable Memory Encryption Mechanism with Optimized Metadata Structure

Rei Ueno  
Tohoku University  
Sendai, Japan  
rei.ueno.a8@tohoku.ac.jp

Hiromichi Haneda  
Tohoku University  
Sendai, Japan  
hiromichi.haneda.r5@dc.tohoku.ac.jp

Naofumi Homma  
Tohoku University  
Sendai, Japan  
naofumi.homma.c8@tohoku.ac.jp

Akiko Inoue  
NEC  
Kawasaki, Japan  
a\_inoue@nec.com

Kazuhiko Minematsu  
NEC  
Kawasaki, Japan  
k-minematsu@nec.com

## ABSTRACT

This study presents an efficient recoverable memory encryption mechanism, named Crystalor. Existing memory encryption mechanisms, such as Intel SGX integrity tree, offer neither crash consistency nor recoverability, which results in attack surfaces and causes a non-trivial limitation of practical availability. Although the crash consistency of encrypted memory has been studied in the research field of microarchitecture, existing mechanisms lack formal security analysis and cannot incorporate with metadata optimization mechanisms, which are essential to achieve a practical performance. Crystalor efficiently realizes provably-secure recoverable memory encryption with metadata optimization. To establish Crystalor with provable security and practical performance, we develop a dedicated universal hash function PXOR-Hash and a microarchitecture equipped with PXOR-Hash. Crystalor incurs almost no latency overhead under the nominal operations for the recoverability, while it has a simple construction in such a way as to be compatible with existing microarchitectures. We evaluate its practical performance through both algorithmic analyses and system-level simulation in comparison with the state-of-the-art ones, such as SCUE. Crystalor requires 29–62% fewer clock cycles per memory read/write operation than SCUE for protecting a 4 TB memory. In addition, Crystalor and SCUE require 312 GB and 554 GB memory overheads for metadata, respectively, which indicates that Crystalor achieves a memory overhead reduction of 44%. The results of the system-level simulation using the gem5 simulator indicate that Crystalor achieves a reduction of up to 11.5% in the workload execution time compared to SCUE. Moreover, Crystalor achieves a higher availability and memory recovery several thousand times faster than SCUE, as Crystalor offers *lazy recovery*.

## KEYWORDS

Memory encryption, Secure computer architecture

## 1 INTRODUCTION

### 1.1 Background

Memory encryption is an essential security primitive for modern computers. Owing to extensive attacks on main memory, including the cold boot attack, Rowhammer, and RAMbleed [28, 37, 41],

which pose real threats, memory encryption is becoming increasingly relevant in a wide range of computers. Trusted execution environment (TEE) mechanisms, such as Intel software guard extension (SGX) and ARM secure encrypted virtualization (SEV), support main memory (DRAM) encryption for realizing resource isolation, remote attestation, *etc.* Moreover, non-volatile memory and persistent memories (NVMs), such as MRAM [19], have been deployed and have attracted substantial attention. In several recent systems, NVMs have been deployed as main memory in addition to or instead of DRAM for higher performance, lower power consumption, and larger capacity, such as NVDIMM and Intel Optane Persistent Memory [2]. Attacks on main memory are more serious and realistic for NVM than DRAM owing to the non-volatility. With the advances in large-scale (persistent) memories, a high demand exists for the development of efficient memory encryption mechanism for the security of modern and future computers.

**Conventional security notions.** Memory encryption realizes the confidentiality (privacy) and/or authenticity (integrity) of main memory data based on symmetric cryptography, including encryption, authenticated message code (MAC), and authenticated encryption (AE) [25]. In [6], Avanzi *et al.* classified and formalized memory protection into three levels:

- L1: confidentiality only,
- L2: confidentiality and integrity,
- L3: confidentiality, integrity, and replay protection.

For example, AMD–SEV employs AES–XEX for memory encryption [1], corresponding to L1. As well, the Optane module is equipped with a 256-bit AES–XTS engine for data privacy without authenticity. However, authenticity is currently considered as essential for protecting main memory, as some practical attacks have been reported that exploit the lack of (full) authenticity of encrypted memory (*e.g.*, ciphertext-based side-channel attacks) [12, 44–46, 55–57, 76, 79]. Here, replay attack, which involves a data move in the time domain (*i.e.*, copy-and-paste of data from past timing), is sophisticated manipulation/forgery. Replay attack cannot be prevented by the simple use of encryption and MAC (*i.e.*, L2 security), as the manipulated data had been originally valid. Hence, many studies have been devoted to the realization of L3 security, which considers the strongest adversary counteracted by memory encryption (*i.e.*, an active but non-invasive hardware attacker  $\mathcal{A}_{\text{active}}^{\text{HW}}$  [6]), from both cryptographic and microarchitectural perspectives [15, 17, 22, 25,

26, 31, 34, 43, 81]. For example, Intel SGX memory encryption, based on the SGX integrity tree (SIT), achieves L3 security [15].

**Memory authentication trees.** For an L3 memory encryption, Merkle tree [52, 53] (in combination with an encryption of leaf nodes) and parallelizable authentication tree (PAT) [29] have been developed for protection against extensive attacks with a realistic computational latency. SIT is a popular PAT instance [15, 25, 26]. Each leaf node consists of encrypted data, a counter value (*i.e.*, nonce), and a verification tag, whereas each intermediate/root node consists of a nonce and a tag to verify its child node as security metadata. When reading (*resp.* storing) data in a leaf node, all nodes on the path from the leaf to root nodes are verified (*resp.* updated). Such a tree structure enables real-time processing of verification and update because its path verification is far faster than the MAC computation for the entire memory. In addition, the root node, which consists of only several hundred bits, is stored on-chip, as the attacker supposedly cannot manipulate on-chip data. Thus, the root node acts as a root of trust to preclude replay attacks.

**Crash consistency.** The aforementioned L3 security has been considered as a sufficiently strong goal in the plain model; however, *it is insufficient for the practice of memory encryption*. For sound availability, memory data should guarantee *crash consistency*: the data are not broken after a crash (*e.g.*, sudden power-off/blackout) occurs [49]. For this purpose, a write pending queue (WPQ) is employed in CPUs as an asynchronous DRAM refresh (ADR) domain to persist data to be stored in main memory. For encrypted memory based on Merkle tree or PAT, however, it is mandatory to guarantee the consistency of all data, including metadata of intermediate nodes. If a tag verification (on intermediate nodes) fails, the related data (leaf node) becomes unavailable because it may have been manipulated. However, it is non-trivial to guarantee crash consistency of the entire tree because a path is to be updated serially in practice (although the computation may be parallelized [29]). This is called *crash window* problem [32]: there must exist a moment when a path is inconsistent (*i.e.*, some nodes are updated while others are not yet). Thus, it is challenging to efficiently guarantee consistency against crashes whenever the system operates.

**Attack on availability.** The security (*i.e.*, confidentiality and integrity) of PAT has been proven [29, 34] in the adversarial model in which the attacker (intentionally) causes crashes and queries inconsistent trees. However, the crash consistency suggests an additional security issue with respect to availability. A malicious attacker may mount a type of denial-of-service (DoS) attack by injecting error(s) into the tree nodes, which makes the related data unavailable<sup>1</sup>. In addition, such faults can be accidentally injected owing to, for example, soft errors. In contrast, the existing crash consistency mechanisms (see Section 1.4) can neither correct the errors (not owing to crash) nor recover the memory with integrity. Thus, the L3 memory encryption significantly degrades availability against malicious attackers and faults, and it is quite important to develop how to maintain the availability of encrypted memory<sup>2</sup>.

<sup>1</sup>Although some memories are equipped with an error-correcting code (single error correction and double error detection (SECDED)), it offers neither correction/detection capabilities nor security against malicious attackers.

<sup>2</sup>We stress that any mechanism cannot always recover the data if encrypted payload data (*i.e.*, contents unrelated to the tree structure) is compromised. Our proposed mechanism can incorporate with error correction code(s) and *tagged/colored memory* [20, 27, 42, 58, 68], which offer an error correction in main memory (encrypted

**New security notion and our motivation.** Given the above observations, we introduce a new security level for memory encryption:

- L4: confidentiality, integrity, replay protection, and recoverability.

An encrypted memory is recoverable if the payload data can be recovered against any manipulation and error (except for leaf nodes) in addition to crash. The L4 security considers the adversary as in the L3 security (*i.e.*,  $\mathcal{A}_{\text{active}}^{\text{HW}}$ ), but achieves a higher availability and resilience against faults and DoS attacks than L3 memory encryption. The goal of this study is to develop an efficient and recoverable memory encryption mechanism that achieves L4 security for the practice of memory encryption. Note that the crash consistency is *not* equivalent to recoverability, as crash-consistent (but not recoverable) memory encryption may not support a recovery but only supports detection when data are manipulated.

## 1.2 State-of-the-art and its limitations

Crash consistency has been studied in the research field of microarchitecture (see Section 1.4), but little formal and provable security analysis has been conducted. In HPCA 2023, Huang and Hua presented a state-of-the-art crash recovery mechanism for L3-secure PAT, named *shortcut update (SCUE)* [32]. SCUE exploits a simple property of naïve PAT metadata; that is, a parent node counter is always equal to the sum of the child node counters. SCUE requires almost no overhead when applied to a PAT-based secure memory, and is currently the most efficient for L4 memory encryption.

However, SCUE has two major limitations in terms of provable security and compatibility with existing optimization mechanisms. SCUE is based on a property of counters in a naïve PAT *without optimization*. Meanwhile, several PAT structural optimizations using advanced counter mechanisms to compress security metadata have been presented, which significantly reduce the memory encryption overhead. *Split Counter (SC)* is the most typical advanced counter mechanism [80], followed by, *e.g.*, *Vault* [71] and *Morphable Counters* [67]. As the metadata overhead has a significant impact on the latency of memory read/write operations owing to the limited bandwidth and cache size, the adoption of such optimizations is crucial for efficient memory encryption. However, SCUE cannot incorporate such structural optimizations using advanced counter mechanisms, which do not preserve the aforementioned simple property of counters. Other major crash consistency mechanisms are also incompatible with these optimizations [88].

Indeed, *combination of recoverable memory encryption and such optimization techniques have rarely been studied and exploited to date, and a mismatch exists between them*. In addition, as the SCUE does not support a lazy/partial recovery (that is, it requires a reconstruction of the *full tree* at a recovery), the availability should be maintained in a more efficient manner. Owing to the advantages of optimization techniques, it is important for the deployment of

payload data). However, their error correction capability is necessarily bounded, and attacker may manipulate leaf node(s) beyond it. Here, although compromised leaves are no longer available, the authentication tree suppresses the unavailability against manipulation/error as payload data encryption is fine-grained into small leaf nodes. In contrast, unless recoverability, one manipulation/error makes all memory data unavailable. Thus, recoverability of authentication trees is essential for practical memory encryption, in addition to error correction codes and tagging/coloring for memory.

secure main memory to develop a recoverable memory encryption mechanism for PAT compatible with optimizations.

### 1.3 Our contributions

We propose a recoverable memory encryption mechanism, named *Crystalor*, which stands for *CRYptographically Secure Tree-based Authentication with Leaf-Only Recovery*. Crystalor efficiently supports the recoverability with almost no latency overhead and is designed to be securely instantiated with any memory authentication tree, including optimized PAT. Crystalor enables an L4-secure memory encryption on the basis of an L3-secure PAT, while our L4-secure memory encryption is compatible with structural optimizations. Meanwhile, as Crystalor incurs almost no latency overhead for the recoverability, our L4-secure memory encryption achieves as efficient performance as that of L3-secure ones.

Our core concepts are twofold. First, Crystalor does *not* guarantee the consistency/recovery of the entire tree but guarantees the integrity and recovery of only leaf nodes (*i.e.*, payload data) using a distinct verification tag, named recovery tag. Second, at a recovery, Crystalor relinquishes the tree except for leaf nodes and creates a new tree from the leaf nodes with resilience against replay attacks. In Section 3, we present our key observations: (1) an almost universal (AU) hash function [14] is sufficient for provably secure recovery tag verification, and (2) it is possible to build an efficient AU hash function with two properties, namely rate-1 (*i.e.*, one block cipher calls to process one input block) and incremental update capability. Accordingly, we develop a (computational) AU hash function named PXOR-Hash, which is tailor-made for our purpose. PXOR-Hash is designed similarly to PXOR-MAC, which is used in the state-of-the-art PAT named ELM [34]; however, PXOR-Hash achieves another security goal/level that we set and has a construction different from PXOR-MAC, which yields efficient implementation<sup>3</sup>. In addition, the recoverability of Crystalor is based on the cryptographic protection, which enables *lazy recovery*. The L4-secure memory encryption based on Crystalor achieves a higher availability than conventional ones thanks to the lazy recovery.

The performance advantage of Crystalor is evaluated by algorithmic analyses and a system-level simulation. Our results reveal that, for protecting a 4 TB memory as an example, Crystalor achieves 29–62% latency reduction per memory read/write in the algorithmic level and a 44% reduction in memory overhead compared to SCUE owing to the compatibility with SC. The system-level simulation using the gem5 simulator [10] shows that Crystalor achieves at most 11.5% lower latency than SCUE. In addition, Crystalor achieves a recovery that is several thousand times faster (*i.e.*, a recovery cost reduction by 90–99.9%) than SCUE owing to the lazy recovery.

### 1.4 Related works

**PAT vs. Merkle tree.** In PAT, the MAC tags on a path can be updated in parallel. PAT enables algorithmically lower latency than

<sup>3</sup>Note that our major contribution includes presenting an L4-secure memory encryption mechanism with how to use cryptographic primitives to realize a secure and recoverable memory and its concrete construction, rather than development of new proof technique or refreshingly new cryptographic primitive. We developed Crystalor with a simple construction to leverage the existing cryptographic theories and for the compatibility with existing architectures and optimization mechanisms.

Merkle tree because the path update of Merkle tree is not parallelizable. Although Merkle tree realizes crash recovery more easily than PAT [32, 88], realizing a leaf recovery under fault/manipulation (of even intermediate nodes) remain difficult. In this study, we develop an efficient recoverable mechanism of PAT, which is promising for improving the memory encryption.

**Crash consistency of encrypted memory.** In [85], Mao *et al.* presented *Osiris*, which recovers the tree only from counter values by exploiting error-correcting code bits equipped with memory. In [82], Yang *et al.* presented *cc-NVM*, which caches flushed counter values in WPQ and employs a MAC, in contrast to *Osiris*. In [7], Awad *et al.* presented *Triad-NVM* for the recovery of Merkle tree, which reconstructs the tree from flushed nodes. In [88], Zubair and Awad presented *Anubis*. It uses a *shadow table* stored in memory, which contains information on cached nodes and identifies and recovers non-updated nodes. *Anubis* offers rapid recovery as well as lazy recovery; however, it does not work with metadata optimizations and incurs a non-trivial latency overhead for the shadow table protection. In [3], Alwadi *et al.* presented *Phoenix*, which combines *Osiris* and *Anubis*. In [81], Yang *et al.* presented *ShieldNVM*, which introduces an epoch-based mechanism to aggressively cache the metadata with the consistency preserved. In [31], Huang and Hua presented *STAR* to achieve a reduction in the write overhead and fast recovery. It exploits SIT lazy scheme and instant persistency for modifications in the cache. In [89], Zubair *et al.* investigated the error sensitivity of metadata in Merkle tree and presented *Soteria* to tolerate the errors by its lazy duplication.

**Advanced mechanisms for metadata optimization.** The SC, which is the pioneering advanced counter mechanism [80], compresses and optimizes the tree/metadata structure by splitting nonce counters into major and minor counters. In [71], Taassori *et al.* presented *Vault*, which adjusts the tree arity to reduce the frequency of counter overflow and improve the capacity of the covered region. In [67], Saileshwar *et al.* presented *Morphable counters*, which dynamically/adaptively determines the structure of major and minor counters in SC, and enables to cache more counters in a line. In [87], Zhou *et al.* presented *Lelantus*, which improves the counter-mode AES-based secure memory by exploiting fine-granularity copy-and-write operations. In [21], Freij *et al.* presented *Bonsai Merkle Forest*, which divides a Merkle tree into subtrees.

### 1.5 Paper organization

Section 2 introduces the persistent memory encryption and secure memory. Section 3 outlines the proposed crash recovery mechanism Crystalor, and explains its hardware architecture and operation. Section 4 presents the algorithm-level evaluation regarding SC and a system-level simulation using the gem5 simulator. Finally, Section 5 concludes this paper.

## 2 PRELIMINARIES

### 2.1 System and threat models of memory encryption

Figure 1 shows a system model with memory encryption, which is simplified, but follows many existing studies and is based on a formalization in [6, 25]. We here omitted CPU core(s) to focus on our interest. The model separates the memory system into two areas:

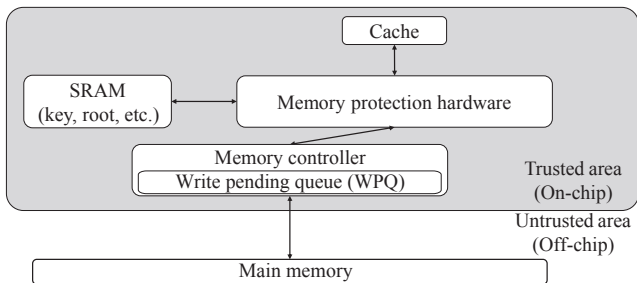


**Figure 1: System model of encrypted memory (CPU core(s) are omitted).**

the on-chip trusted area and the off-chip untrusted area. On-chip data are assumed to be secure and trustable; that is, any attacker can *neither* eavesdrop nor manipulate on-chip data. In contrast, he/she can perform arbitrary eavesdropping/manipulation of off-chip data. The goal of memory encryption is to realize the confidentiality and integrity of memory data. Thus far, block cipher (*e.g.*, AES) has been used for confidentiality, and MAC (*e.g.*, HMAC) is for integrity (*i.e.*, the detection of data manipulation/forgery) [22]. The on-chip area contains cache(s), memory protection hardware, SRAM, and a WPQ. The SRAM stores the secret key and root nonce of PAT. The memory protection hardware performs cryptographic computation (*i.e.*, encryption/decryption and MAC). The CPU systems employ a WPQ as an ADR domain to buffer data from the cache to memory until it is written, which guarantees the data persistency at the time of cache data replacement/flush. This threat model is compatible with many existing studies on memory encryption [22, 25, 32] and corresponds to the strongest adversary covered by memory encryption (*i.e.*,  $\mathcal{A}_{\text{active}}^{\text{HW}}$  formalized in [6]).

*Remark 2.1* (Side-channel attacks). We do not consider on-chip side-channel attacks as in previous studies. For example, power, EM, timing, and cache analyses on cryptographic primitives may steal the secret key [39, 40, 72, 73]. Microarchitectural attacks represented by Flush+Reload and Prime+Probe [48, 83], which are exploited by Spectre and Meltdown [38, 47], may also be a threat to the confidentiality of payload data. These side-channel attacks are attempts to eavesdrop and manipulate *on-chip* data. Hence, they are beyond our scope: protection of *off-chip* data against eavesdropping and manipulation. On-chip side-channel attacks should be countered by different means, such as masking [24, 51] and cache randomization [13, 62, 63, 78] (although an authentication tree named MEAS claims a power/EM side-channel security [75]).

## 2.2 Symmetric cryptography for memory encryption

Existing works on memory encryption (*e.g.*, [17]) have frequently employed AES encryption. For confidentiality, the counter-mode AES has been utilized owing to its parallelizability and random accessibility. A nonce is also used for the encryption as security metadata, which is composed of a memory address and counter. For integrity, a MAC has been commonly employed in PAT. Note here

that replay attacks cannot be prevented by simple use of MAC, because they manipulate data using a valid tuple of ciphertext, nonce, and tag, which motivates the use of PAT for memory encryption.

Recently, for encrypting and verifying payload data, some state-of-the-art PATs, such as ELM [34], utilize an authenticated encryption (AE) [64] for leaf nodes instead of a composition of the counter-mode AES encryption and a MAC [9]. For efficient memory encryption, AE should have two desirable properties: block-level parallelizability<sup>4</sup> and rate-1. A parallelizable AE can encrypt several blocks in parallel, which allows for low-latency implementation using a multicore or pipelining. Rate-1 relates to the number of AES calls to complete the encryption and tag computation. A rate-1 AE (*e.g.*, [66]) has a latency of almost half of a composition of the counter-mode AES encryption and a MAC. The use of AE significantly improves the performance of memory encryption, where payload data essentially requires both confidentiality and integrity.

Parallelizability and rate-1 are also desirable for MAC to achieve the integrity of intermediate nodes. In addition, certain MACs have another desirable property known as incrementality [8]. When a data block is changed, an incremental MAC can update the tag with  $O(1)$  calls of the underlying cryptographic primitive using the old data block and tag, whereas typical non-incremental MAC, such as CMAC [18], requires  $O(m)$  primitive calls, where  $m$  is the number of input blocks. The tag of incremental MAC can be updated only from an old tag, old data block, and new data block, as well as old and new nonces. In a path update, the number of blocks updated in a MAC computation is usually one; hence, incremental MAC significantly improves the performance of memory encryption.

## 2.3 Parallelizable authentication tree (PAT)

PAT has been employed for memory encryption to realize (1) real-time processing and (2) protection against replay attacks with a minimal overhead of on-chip memory. Figure 2 depicts an overview of PAT with an arity of two as an example. The PAT encrypts the leaf node using an AE and verifies intermediate nodes using a nonce-based MAC. The  $i$ -th intermediate node of PAT (including the root node) consists of  $(N[i], T[i])$ , where  $N[i]$  and  $T[i]$  are its nonce and tag, respectively. The  $i$ -th leaf node of PAT consists of  $(N[i], T[i], C[i])$ , where  $C[i]$  is the ciphertext of payload data. The nonce of each node is given by a concatenation of its address  $\text{addr}[i]$  and counter  $\text{ctr}[i]$  as  $N[i] = \text{addr}[i] \parallel \text{ctr}[i]$ , where  $\cdot \parallel \cdot$  denotes the bit concatenation<sup>5</sup>. The tag of an intermediate node verifies its child node counters as the MAC input. In both verification and update, the tag of each node in a path is computed in parallel as its computation does not depend on the computation results of any lower-level nodes, which indicates the node-level parallelizability of PAT.

**ELM.** ELM is a state-of-the-art PAT proposed by Inoue *et al.* [34]. ELM is optimized for low latency and scalability to large memory. For this purpose, Inoue *et al.* introduced an AE and incremental MAC named Flat-OCB and PXOR-MAC, respectively. In addition, ELM unifies some computations shareable with Flat-OCB and PXOR-MAC among the entire tree. ELM has a lower latency and

<sup>4</sup>Block-level parallelizability is a property of the mode and MAC, whereas node-level parallelizability is of the authentication tree.

<sup>5</sup>Note that  $\text{addr}[i]$  does not need storing because it is implicitly determined from its physical address [15, 34].

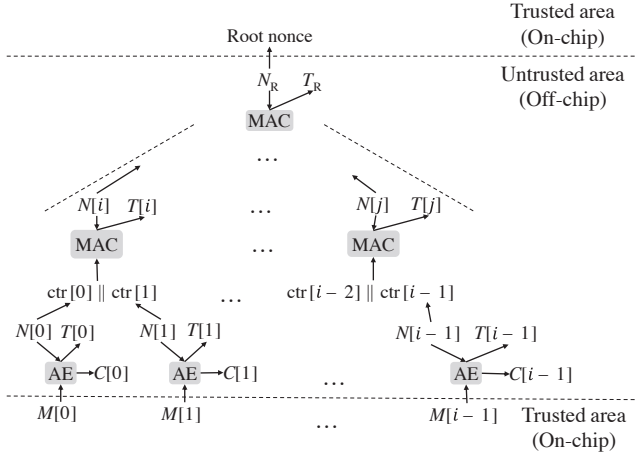


**Figure 2: Overview of binary PAT.**  $M[i]$ ,  $C[i]$ ,  $N[i]$ , and  $T[i]$  denote plaintext (*i.e.*, payload data), ciphertext, nonce, and tag of  $i$ -th node, respectively, where  $N[i]$  consists of address  $\text{addr}[i]$  and counter  $\text{ctr}[i]$ .  $N_R$  and  $T_R$  are root nonce and tag, respectively. Leaf node is defined as  $(N[i], T[i], C[i])$ , whereas other nodes are defined as  $(N[i], T[i])$ .

less memory overhead than SIT [15], while both schemes use AES-128 and have an equivalent provable security reduction to AES. Notably, several major previous studies on memory encryption (*e.g.*, [22, 32]) employed a classical HMAC, which has a larger latency owing to its serial structure and does not have incrementality. The MAC of ELM (and SIT) is significantly faster than the HMAC.

## 2.4 Shortcut update (SCUE)

SCUE is a state-of-the-art recoverable memory encryption mechanism with PAT presented by Huang and Hua in HPCA 2023 [32]. In SCUE, the counter of the nonce in PAT is *incremented by one* whenever the node is updated and never decreases under nominal operation (without any reset nor overflow). Its security against replay relies on the fact that a replay attacker can decrease a counter of a node by replacing the nonce and tag in the past but cannot increase it, yet no formal security analysis has been conducted.

The proposals of SCUE include (i) the efficient integrity verification of leaf nodes and (ii) the reconstruction of intermediate nodes from the leaf nodes. The basic concepts underlying SCUE are that, unless any manipulation, (i) the root counter is always equivalent to the sum of all leaf counters, and (ii) a parent node counter is always equivalent to the sum of its child node counters. These facts are apparent because the counter represents the number of node updates. After a crash, the integrity of leaf nodes is first verified using the AE/MAC with the tag and nonce stored in memory. Assuming the security of AE/MAC, the attacker cannot perform any forgery except for replay. Subsequently, to detect a replay of leaf nodes, the SCUE checks the equivalence between the root counter and the sum of leaf counters. Here, the root counter is manipulation-free because it is on-chip. In addition, a replay decreases a counter but cannot increase it, indicating that the sum of leaf counters must be fewer than the root counter if replayed.

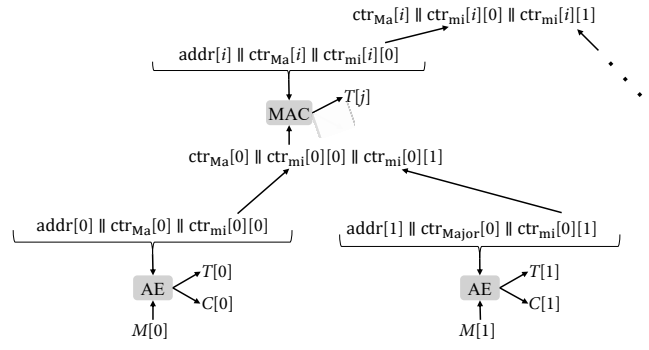


**Figure 3: Example of SC-based binary PAT, where  $\text{ctr}_{\text{Ma}}[i]$  is  $i$ -th major counter, and  $\text{ctr}_{\text{mi}}[i][j]$  is  $j$ -th minor counter sharing  $\text{ctr}_{\text{Ma}}[i]$ . MAC input of parent node consists of major counter(s) and all minor counters of child nodes.**

Following the verification, SCUE recovers the intermediate nodes before the crash in a bottom-up manner. It determines each parent node counter value as the sum of its child node counters because they are always equivalent unless manipulation.

## 2.5 Split Counter (SC)

SC is the foremost advanced counter mechanism for PAT structural optimization [80], which compresses the tree size (*i.e.*, suppresses the memory overhead for metadata) [5, 60, 61]. This contributes to reduction of the amount of communication between memory and CPU as well as lower latency of AE/MAC computation.

Figure 3 illustrates an overview of an SC-based PAT with an arity of two. An SC-based tree splits a counter into major and minor counters. Minor counter is unique to a node, while major counter is shared by several nodes. In computing AE for a leaf node, the nonce is determined by a concatenation of its address, its major counter, and its minor counter (*e.g.*,  $\text{addr}[0] \parallel \text{ctr}_{\text{Ma}}[0] \parallel \text{ctr}_{\text{mi}}[0][0]$  in Figure 3) and the input (*i.e.*, data to be encrypted/decrypted and verified) is the payload data (*e.g.*,  $M[0]$ ). In computing MAC of an intermediate or root node, the nonce is determined by its address, its own major counter, and its own minor counter (*e.g.*,  $\text{addr}[i] \parallel \text{ctr}_{\text{Ma}}[i] \parallel \text{ctr}_{\text{mi}}[i][0]$ ) and the input (*i.e.*, data to be verified) is a concatenation of the major counter(s) and all corresponding minor counters of its child node (*e.g.*,  $\text{ctr}_{\text{Ma}}[0] \parallel \text{ctr}_{\text{mi}}[0][0] \parallel \text{ctr}_{\text{mi}}[0][1]$ ). In updating a node, its minor counter is incremented. Here, if a minor counter overflows, then all minor counters that share a major counter are reset to zero, and the major counter is incremented. Thus, the SC significantly reduces the total bit length of the counters, thereby maintaining the uniqueness of the nonce.

Let  $l_{\text{ctr}}$  be the bit length of the counter without SC. Let  $l_{\text{Ma}}$  and  $l_{\text{mi}}$  be those of the major and minor counters of an SC-based PAT, respectively. Typically,  $l_{\text{ctr}}$ ,  $l_{\text{Ma}}$ , and  $l_{\text{mi}}$  are 64, 56, and 8, respectively [33, 80]. If  $k$  nodes share a major counter, SC reduces the counter size from  $kl_{\text{ctr}}$  to  $l_{\text{Ma}} + kl_{\text{mi}}$ .

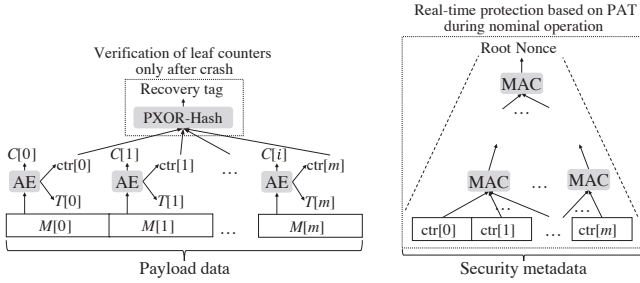


Figure 4: Secure memory based on PAT and Crystalor.

### 3 PROPOSED MECHANISM: CRYSTALOR

#### 3.1 Basic concept of Crystalor

Figure 4 depicts the proposed L4-secure memory encryption named Crystalor based on PAT. Crystalor distinctly provides crash recoverability and security against crashes, while PAT solely provides confidentiality and integrity *under nominal operation without a crash*. The basic concepts of Crystalor are the use of a distinct *recovery tag*, which verifies the leaf node integrity *only after a crash* but can be updated with almost no overhead under nominal operations, and to construction of a new tree with a proven resilience against replay following the recovery tag verification.

Our idea is based on the fact that, if we can verify the leaf nodes (*i.e.*, payload data) regarding replay attacks without intermediate node consistency, the intermediate node is no longer required. Thus, we disregard the entire tree consistency and relinquish the intermediate and root nodes. Crystalor realizes the leaf node verification using the recovery tag stored on-chip. The recovery tag verification is only performed after a crash or verification failure, while PAT provides integrity under nominal operation. This indicates that the recovery tag verification does not require real-time processing. In contrast, the tag update requires real-time processing because it should be performed whenever storing data. Thus, we present an incremental universal hash [14] named PXOR-Hash, which is tailor-made for an efficient and optimal realization of such recovery tag. PXOR-Hash is designed similarly to PMAC (and PXOR-MAC); however, PXOR-Hash and PMAC achieve different security goals/levels owing to the difference in their contexts (see Section 3.2), which enables PXOR-Hash to improve the efficiency and latency compared to PMAC. Importantly, PXOR-Hash verifies any data regardless of its structure, which enables the integrity verification of PAT with structural optimizations (in contrast to SCUE).

The proposal of Crystalor includes how to rebuild the entire tree (*i.e.*, intermediate nodes) from the verified leaf nodes. Recovery of an SC-based PAT is impossible because minor counter values at overflow are discarded, which causes uncertainty on the intermediate counters. In contrast to existing mechanisms, Crystalor creates a new tree, where resilience against replay attacks is proven.

#### 3.2 Recovery tag verification using PXOR-Hash

AE can verify leaf nodes (*i.e.*, payload data) with a nonce consisting of its address and counter. Here, as we use an implicit (*i.e.*, physical) address for the nonce, we can detect a forgery, including splicing, but not a replay attack on a leaf node. To detect a replay, we should

verify the integrity of counters using a recovery tag stored on-chip securely. As the recovery tag is verified only after a crash, only its update requires real-time processing (whereas its verification does not). The requirements of recovery tags for security and practical performance are as follows.

**Requirement 1 (Security).** Let  $F$  denote a function that computes an  $n$ -bit recovery tag from input  $D$ , which consists of leaf counter blocks. For any adversary with practical resources, the probability of finding a collision on  $F$  (*i.e.* a distinct pair  $D$  and  $D'$  such that  $F(D) = F(D')$ ) is negligible in  $n$ .

**Requirement 2 (Incremental update).** Assume that old tag and old input blocks are available. If one input block is changed, then the new tag can be computed with  $O(1)$  calls of symmetric cryptographic primitive. Note that this assumption is generally true in our context because old data remains on-chip before the update.

**Requirement 3 (Fast recovery).** The tag can be computed and verified with  $m + O(1)$  calls of symmetric cryptographic primitive (*i.e.*, rate-1), where  $m$  is the input length.

Requirement 1 is crucial as it directly represents a forgery of a recovery tag given an input (*i.e.*, leaf node counters). The function  $F$  is either keyed or unkeyed. In the former case, we assume that the adversary does not know the (random) key, owing to the availability of on-chip key register. Here, if  $F$  is keyed, Requirement 1 is equivalent to requiring  $F$  to be an almost universal (AU) hash function (See Definition 1) [14]. AU hash functions have been extensively studied, which can be efficiently constructed owing to the secret key dependency, compared to one-way hash functions such as SHA-2 or SHA-3.

For a keyed function  $F : \mathcal{K} \times \mathcal{X} \rightarrow \mathcal{Y}$  where  $\mathcal{K}$  is the key space, we write  $F_K$  to denote  $F(K, \cdot)$ .

**Definition 1 (AU hash function).** Let  $F : \mathcal{K} \times \mathcal{D} \rightarrow \{0, 1\}^n$  be a function for a key  $K \in \mathcal{K}$  and plaintext  $D \in \mathcal{D}$ . The function  $F$  is an  $\epsilon$ -AU hash function if  $\Pr[K \leftarrow \mathcal{K} : F_K(D) = F_K(D')] \leq \epsilon$  holds for any  $D$  and  $D' \in \mathcal{D}$  such that  $D \neq D'$ .

We remark that a full-fledged (nonce-based) MAC will also work; however, an AU hash function is sufficient for our purpose. This is because, in our architecture, the recovery tag is stored in the on-chip trusted/secure area, where *the adversary in Requirement 1 cannot see nor manipulate it*. This feature is crucial because a collision is usually easy to find if the output of the AU hash is visible to the adversary. A nonce is unnecessary because *each leaf node counter is never repeated under nominal operation*. If the recovery tag was stored off-chip or the plaintext of  $F$  could take the same value, we would need to employ a conventional MAC, or add a nonce as a new input of  $F$  and employ nonce-based MAC. However, this will increase the computational cost or latency compared to an AU hash function. Based on these observations, we develop an AU hash function PXOR-Hash, which fulfills these three requirements. Although an AU hash function could be built using algebraic operations (*e.g.*, GHASH in GCM), such constructions have difficulties in incremental updates for large inputs. Instead, we adopt a computational variant of AU hash function, which is a simplified version of PMAC (*i.e.*, the sum of input-masked AES). This enables incremental updates for large inputs and provable security guarantee based on the symmetric primitive that we use (namely, AES) [65].

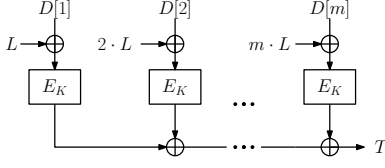


Figure 5: Block diagram of PXOR-Hash.

<b>Algorithm TagGen</b> ( $D, K, L$ ) 1 $T \leftarrow 0^n$ 2 <b>for</b> $i = 1$ to $m$ 3 $T \leftarrow E_K(i \cdot L \oplus D[i]) \oplus T$ 4 <b>return</b> $T$	<b>Algorithm Verify</b> ( $D, K, L, T$ ) 1 $T' \leftarrow \text{TagGen}(D, K, L)$ 2 <b>if</b> $T = T'$ 3 <b>return</b> $\top$ 4 <b>else</b> 5 <b>return</b> $\perp$
<b>Algorithm Update</b> ( $D[i], D'[i], i, K, L, T$ ) 1 $T \leftarrow E_K(i \cdot L \oplus D[i]) \oplus T$ 2 $T \leftarrow E_K(i \cdot L \oplus D'[i]) \oplus T$ 3 <b>return</b> $T$	

Figure 6: PXOR-Hash algorithms, where  $D = (D[1], D[2], \dots, D[m])$  and  $D'[i]$  is new data to be updated.

**Construction of PXOR-Hash (for Requirement 3).** Let  $E_K(\cdot)$  denote a block cipher encryption using a secret key  $K$  (typically,  $E_K$  is AES encryption). Let  $D[1], D[2], \dots, D[i], \dots, D[m]$  be input data blocks to be verified, where  $m$  is the number of data blocks. In the context of Crystalor, each  $D[i]$  consists of counters for a leaf node nonce (see below). Figure 5 and Figure 6 show the block diagram and algorithmic description of PXOR-Hash, respectively. The tag of PXOR-Hash is computed as

$$T = E_K(L \oplus D[1]) \oplus E_K(2 \cdot L \oplus D[2]) \oplus \dots \oplus E_K(i \cdot L \oplus D[i]) \oplus \dots \oplus E_K(m \cdot L \oplus D[m]),$$

where  $L = E_K(0)$ , the operator  $\oplus$  denotes a bit-wise XOR, and the multiplication is over  $\mathbb{F}_{2^n}$  ( $n$  is the block length of  $E_K$ ). Note that  $L$  can be pre-computed and stored in on-chip memory in advance to remove its latency. Obviously, the tag is computed with  $m$  calls of  $E_K$ , which means rate-1.

**Incremental update (for Requirement 2).** Given an old tag  $T$ , let us consider updating the  $i$ -th block  $D[i]$  to  $D'[i]$ . The new tag is expressed as

$$T' = E_K(L \oplus D[1]) \oplus E_K(2 \cdot L \oplus D[2]) \oplus \dots \oplus E_K(i \cdot L \oplus D'[i]) \oplus \dots \oplus E_K(m \cdot L \oplus D[m]). \quad (1)$$

Using the old tag  $T$  and old data  $D[i]$ , the new tag  $T'$  is equivalently computed as

$$T' = T \oplus E_K(i \cdot L \oplus D'[i]) \oplus E_K(i \cdot L \oplus D[i]), \quad (2)$$

which requires only two  $E_K$  calls, whereas the naïve computation in Equation (1) requires  $m$  calls.

**Concrete realization.** For the leaf node verification, we compute and store a recovery tag  $T$  using PXOR-Hash on-chip, where the inputs are  $\text{ctr}[1] \parallel \text{ctr}[2] \parallel \dots \parallel \text{ctr}[m]$ . We use AES-128 for a block cipher, and 64-bit counters (without SC). The input data are expressed as  $D[i] = \text{ctr}[2i] \parallel \text{ctr}[2i+1]$  for each  $1 \leq i \leq m$ . If the  $2i$ - or  $(2i+1)$ -th node is updated, then  $D[i]$  is also updated using the computation in Equation (2). Also, if we use SC, the  $i$ -th input

data block is given by all node counters related to the  $i$ -th major counter; that is,  $D[i] = \text{ctr}_{\text{Ma}}[i] \parallel \text{ctr}_{\text{mi}}[i][0] \parallel \text{ctr}_{\text{mi}}[i][1] \parallel \dots \parallel \text{ctr}_{\text{mi}}[i][k]$ , where  $k$  is the number of minor counters. If a leaf node related to  $\text{ctr}_{\text{Ma}}[i]$  and  $\text{ctr}_{\text{mi}}[i][1], \text{ctr}_{\text{mi}}[i][2], \dots, \text{ctr}_{\text{mi}}[i][k]$  is updated, then  $D[i]$  is updated. Note that the address is not required to be input to PXOR-Hash because PXOR-Hash can detect a change in the block order. If a crash occurs, Crystalor first verifies the leaf node using the AE and then detects a replay attack by comparing the on-chip recovery tag and the tag computed by Equation (1).

**Security of PXOR-Hash (for Requirement 1).** As mentioned previously, PXOR-Hash is a computational AU hash function, or more precisely, an almost XOR-universal (AXU) hash function. An AXU hash function is an AU hash function. Note here that, for a leaf node with  $\text{ctr}_{\text{Ma}}[i]$  and  $\text{ctr}_{\text{mi}}[i][j]$ ,  $i$  and  $j$  are implicit inputs to PXOR-Hash (that is, the input order of the major and minor counters, which represents the node address). As PXOR-Hash can detect a swap of bits/blocks, Crystalor is secure against splicing. Thus, PXOR-Hash can detect any manipulation on leaf node counters, if the collision probability is negligible.

Integrity will be lost if the securely stored hash value (*i.e.*,  $T$ ) and output of PXOR-Hash with a modified (forged) input collide. Concretely, the probability for each forgery attempt is at most  $4m/2^n$  when  $m \leq 2^{n-2}$ , where  $n = 128$  and  $m$  is the number of input blocks, assuming that the underlying AES is computationally secure (*i.e.*, a pseudorandom permutation). Hence, the collision probability is negligible in practice if  $m \ll 2^{n-2} = 2^{126}$ . For example, even for a very large memory of 1 P bits, the collision probability is less than  $2^{-83}$ , which is practically negligible. The collision probability of PXOR-Hash can be obtained by analyzing (the message hashing part of) PMAC [65]. Originally the collision probability was at most  $m^2/2^n$  [65]; Minematsu and Matsushima [54, Lemma 2] improved it to  $4m/2^n$ , assuming that  $m \leq 2^{n-2}$ . These proofs considered doubling-based masks, which means that the  $i$ -th input mask is  $2^i \cdot L$ , where “2” denotes the generator of the field  $\text{GF}(2^n)$ . This differs from  $i \cdot L$  in PXOR-Hash as we adopted it for hardware suitability. However, the proof of [54, Lemma 2] is applicable to our case with trivial changes. Hence, we omit the proof here.

If a stronger security bound should, which may occur when  $m$  is even larger, or if the block size is smaller, we can use stronger methods, such as (the message hashing part of) PMAC with multiple masks [23] and TBC-based PHASH [65]. The former could be instantiated low-latency block ciphers such as Prince [11], and the latter could be instantiated with a low-latency TBC such as QARMA [4]. Both methods further reduce the contribution of input length in the collision bound.

### 3.3 Memory recovery by constructing new tree

To date, PAT recovery after a crash has been realized by reconstructing intermediate nodes (*i.e.*, nonce counters) using a redundancy or the relation between parent and child nodes. For example, Anubis uses a shadow table to preserve the node addresses under updates [88]. SCUE reconstructs intermediate nodes from leaf nodes in a bottom-up manner, owing to the consistency between the sum of child node counters and a parent node counter. These existing methods cannot work with SC because minor counter values are discarded and reset when an overflow occurs.

Here, intermediate nodes are not payload data but are only used for verifying leaf nodes regarding a replay attack. In other words, the intermediate nodes are unnecessary if we can verify the leaf nodes in another way (e.g., the recovery tag of PXOR-Hash). Therefore, Crystalor relinquishes the old tree, except for the leaf node, and constructs a new tree. However, if an old counter is used in the new tree, it is exploited by a replay attack, resulting in a feasible forgery. Thus, we should construct a new tree with counter values greater than the old ones for resilience against replay.

We derive an upper bound of the number of updates of a node from its child node counters and propose its use as the new counter value. Consider a case in which  $k$  leaf nodes share a major counter and the minor counter bit length is  $l$ . A parent node has a major counter  $\text{ctr}_{\text{Ma}}[i]$  and a minor counter  $\text{ctr}_{\text{mi}}[i][j]$  for each  $1 \leq j \leq k$ . For a PAT with arity of  $\beta$ , it has  $\beta$  child nodes with major counters  $\text{ctr}_{\text{Ma}}[i']$  and minor counters  $\text{ctr}_{\text{mi}}[i'][j']$  ( $1 \leq i' \leq \beta/k$  and  $1 \leq j' \leq k$ ). After a crash, Crystalor computes the maximum possible number of the parent nodes (i.e., an upper bound), which is denoted by  $\text{ctr}_{\text{ub}}[i][j]$ , as

$$\text{ctr}_{\text{ub}}[i][j] = \sum_{i'=1}^{\beta/k} \left( \text{ctr}_{\text{Ma}}[i'] \left( k(2^l - 1) + 1 \right) + \sum_{j'=1}^k \text{ctr}_{\text{mi}}[i'][j'] \right).$$

Crystalor then computes the major and  $j$ -th minor counter values of the  $i$ -th intermediate node as

$$\text{ctr}_{\text{Ma}}[i] = \sum_{j=1}^k \left\lfloor \frac{\text{ctr}_{\text{ub}}[i][j]}{2^l} \right\rfloor, \quad (3)$$

$$\text{ctr}_{\text{mi}}[i][j] = \text{ctr}_{\text{ub}}[i][j] \bmod 2^l, \quad (4)$$

respectively, where  $\lfloor \cdot \rfloor$  is the floor function. All counters of intermediate and root nodes are computed bottom-up by repeating this computation from the leaf nodes. This is based on a fact that the upper bits of nonce are shared as a major counter while the lower  $l$  bits are unique to each minor counter.

We prove Theorem 1 to validate the security of the recovery of Crystalor against replay attack.

**Theorem 1.** *Let  $\text{ctr}_{\text{Ma}}[i]$  and  $\text{ctr}_{\text{mi}}[i][j]$  be the  $i$ -th parent node major and minor counter values computed by Equations (3) and (4), respectively. Any new tree is resistant to replay attacks.*

**PROOF.** First, we consider a single crash. Let  $c$  be the number of updates from the previous reset of minor counters until the next reset (i.e., major counter increment). It always holds  $2^l \leq c \leq k(2^l - 1) + 1$ , because  $c$  is the minimum if only one node is updated (and the others are not updated at all), whereas  $c$  is the maximum if each of the  $k$  minor counters has the maximum value (i.e.,  $2^l - 1$ ). Let  $u_{i'}$  be the total number of updates of nodes sharing the  $i'$ -th major counter, which is bounded above as

$$u_{i'} \leq \text{ctr}_{\text{Ma}}[i'] \left( k(2^l - 1) + 1 \right) + \sum_{j'=1}^k \text{ctr}_{\text{mi}}[i'][j'],$$

because  $\text{ctr}_{\text{Ma}}[i']$  denotes the number of minor counter resets. Let  $u_{i,j}$  be the number of updates of a parent node with  $\text{ctr}_{\text{mi}}[i][j]$ ,

which is bounded above as

$$u_{i,j} \leq \sum_{i'=1}^{\beta/k} u_{i'} = \text{ctr}_{\text{ub}}[i][j].$$

This indicates that  $\text{ctr}_{\text{ub}}[i][j]$  is greater than or equal to the number of updates of the node (i.e., the true value of the parent counter ever before). The equality holds if  $c$  is the maximum value whenever and wherever the minor counter resets or if any minor counter reset has not occurred (i.e.,  $\text{ctr}_{\text{Ma}}[i'] = 0$  for all  $i'$ ). Thus, for all  $1 \leq j \leq k$ , the parent node is updated at most  $\text{ctr}_{\text{ub}}[i][j]$  times. As  $2^l \leq c \leq k(2^l - 1) + 1$  also holds for the parent node, the number of updates of the parent major counter must be less than  $\sum_{j=1}^k \left\lfloor \text{ctr}_{\text{ub}}[i][j]/2^l \right\rfloor$ , which indicates that the new major counter value never appears before the crash. Thus, its replay is impossible.

Next, we consider multiple crashes, in which the counter values are given by Equations (3) and (4) in the past. If a leaf node counter is incremented, then a corresponding  $\text{ctr}_{\text{ub}}[i]$  always has a greater value than the previous state, because it is strictly monotonically increasing in terms of both  $\text{ctr}_{\text{Ma}}[i']$  and  $\text{ctr}_{\text{mi}}[i'][j']$ . This implies that either or both  $\text{ctr}_{\text{Ma}}[i]$  and  $\text{ctr}_{\text{mi}}[i][j]$  are greater than any previous state. In addition, if a child node is updated, its parent node counter increases accordingly; however, its increase amount is not as great as the number of updates, as aforementioned. Thus, the new counter values determined by Equations (3) and (4) are always new, which guarantees resistance against replay attacks.  $\square$

The integrity of leaf nodes is verified by AE, excluding replay attacks. The recovery tag verification detects the replay attacks on leaf nodes. In addition, Theorem 1 states that the counter values of the new tree are always greater than values before the crash, which indicates the resistance of the new tree to replay attacks. Thus, Crystalor provides both crash recoverability and integrity against any manipulation attacks. Note that, in a recovery operation, the new tree construction and leaf node/tag verification should be carefully executed so as to avoid replay attacks (see Section 3.5).

### 3.4 Hardware architecture

Figure 7 displays the hardware architecture of Crystalor for L4 memory encryption [34], in which we employ ELM. Crystalor utilizes dedicated hardware components to compute and update the recovery tag apart from memory protection hardware for ELM computation, as Crystalor operates distinctly and independently of PAT. The dedicated hardware consists of an SRAM to store and update the recovery tag (Recovery TAG register) in addition to the secret key of PXOR-Hash key (KEY register). PXOR-Hash hardware consists of pipelined AES encryption hardware, which can process multiple update transactions in parallel in the most efficient manner. The recovery tag is stored in both the SRAM and cache (Recovery TAG register and cache) to improve the tag computation speeds. This dedicated hardware operates at every timing of leaf node update (i.e., storing encrypted payload data to memory) to simultaneously and consistently update/store the recovery tag to Recovery TAG register and cache. In Figure 7, the recovery tag is always updated on-chip but is not disclosed to the off-chip memory. This is mandatory for security to prevent any manipulation attack



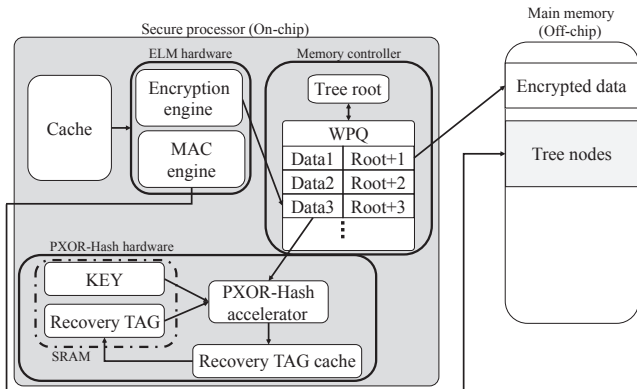


Figure 7: Crystalor hardware architecture.

on these data. In other words, as the recovery tag is securely processed and stored, it does not require as strong protection as MAC, which leads to an efficient implementation of PXOR-Hash.

Crystalor requires on-chip SRAM for storing the 128-bit recovery tag and PXOR-Hash keys ( $K$  and  $L$ ). The SRAM overhead is 384 ( $= 128 \times 3$ ) bits in total. Crystalor also utilizes a 128-bit on-chip cache for Recovery TAG cache and an AES encryption engine for PXOR-Hash, which is implemented with less than 15 K GE [74].

The remaining parts other than Crystalor operate similarly to the conventional ones. A memory controller controls the data flow to handle the encrypted payload data and security metadata. The ELM hardware includes a 952-bit cache for storing the ELM secret key and its precomputable intermediate values. We employ an on-chip WPQ to persist data during store operation using ADR [70]. Namely, as leaf nodes must be consistent with the on-chip recovery tag, we explicitly use a WPQ as an ADR domain for the leaf node to guarantee its persistence at a timing. Note that the intermediate nodes are discarded at a crash; hence, they do not require persistency; thus, the MAC outputs (*i.e.*, intermediate nodes) are directly written to memory without using WPQ (which indicates that the intermediate nodes are computed and updated with background processing like SCUE). Furthermore, we utilize atomic persistency mechanism(s) and hardware redo logging as in existing methods.

*Remark 3.1* (Combination with other mechanisms). Figure 7 presents the simplest construction without any optimization mechanism. Advanced counter mechanisms such as SC, Vault, and Morphable counters are applicable. The adoption of mechanism(s) for atomic data persistency would also be essential for consistent transactions with high performance [16, 30, 35, 36, 50, 59, 69, 77, 84, 86]. As PXOR-Hash operates distinctly from PAT, such optimization mechanisms for PAT can be readily incorporated together.

**Performance overhead.** The latency overhead of Crystalor during nominal operation does *not* depend on the cache size nor covered memory region, but solely depends on the computational cost of the recovery tag update. As mentioned in Section 3.2, the recovery tag update is completed within only two AES encryption calls for new and old  $D[i]$ 's. The two AES encryptions are performed in parallel using pipelined AES hardware, which requires significantly smaller latency of ELM update. Therefore, the latency

overhead is negligible and has no impact on the system performance, as Crystalor and PAT operate distinctly. Crystalor incurs little overhead in the memory controller owing to its simplicity.

### 3.5 Operations

We describe the store and recovery operations of ELM-Crystalor. Read operation requires no Crystalor operation.

**Store operation.** For crash recoverability (covering a crash during AE encryption) and security, we must simultaneously and consistently update the leaf node counter in the memory and the on-chip recovery tag, which is realized by the following steps:

1. Store operation to the memory is issued. It would correspond to a cache data replacement (*i.e.*, cache miss) or an explicit instruction to guarantee the data persistency at a timing, such as `clflush` and `clwb` in x86 architecture.
2. **(ELM computation)** Payload data are encrypted by AE. The MAC tags of the corresponding intermediate nodes and root node tags are computed in the background, and the corresponding counters are incremented on-chip. When AE encryption starts, a busy frag (one-bit on-chip NVM) is raised. AE inputs (*i.e.*, payload data) are preserved in a non-volatile register until the result is moved to WPQ, to achieve recovery from a crash during AE encryption.
3. **(PXOR-Hash computation)** The new recovery tag is computed from the old tag, old data, and new data. This step should be computed in parallel with Step 2.
4. **(Write to WPQ)** The AE encryption result is moved to WPQ. The busy flag is put down when completed.
5. **(Recovery tag update)** Recovery TAG cache and registers are updated.
6. **(Store data)** The WPQ data are stored in memory. This transaction is completed.

Note that Steps (4) and (5) should be synchronously executed in parallel for consistency between the recovery tag and leaf counters. In addition, data should be updated in an atomically persistent manner, with the aid of some mechanisms for this purpose (*e.g.*, [16, 30, 35, 36, 50, 59, 69, 77, 84, 86]).

**Recovery.** Recovery is executed after a crash or upon a verification failure. Crystalor securely recovers the memory as follows:

1. **(AE status check)** If the busy flag has been raised, the AE encryption is performed again using the non-volatile register data and the result is stored to the memory through the WPQ, according to the redo logs.
2. **(New tree construction)** According to Section 3.3, the counter values of intermediate and root nodes are derived in a bottom-up manner. The MAC tag of each node is also computed from the counters and addresses.
3. **(Recovery tag verification)** The recovery tag of PXOR-Hash is computed from all leaf node counters, and then the computed tag is compared to the on-chip Recovery TAG register value. If these are equivalent, the nominal operation restarts; otherwise, Crystalor gives an error signal.

Execution of Steps 2 and 3 in this order prevents any replay. Namely, we create a new tree, although the leaf nodes may be manipulated. Hereafter, PAT can detect any manipulation (while the leaf nodes

are not verified); the attacker cannot perform any manipulation after the new tree construction. Then, we verify the recovery tag to detect replays (and verify the leaf node by AE to detect manipulation after restart as lazy recovery). Thus, All manipulations before the new tree construction are detected by the verifications of recovery tag and the leaf node AE. Contrarily, if we execute Steps 2 and 3 in the reverse order, a replay attack is possible at a timing between the recovery tag verification and the new tree construction.

**Lazy recovery.** Crystalor can detect any counter replay solely by the recovery tag verification, whereas SCUE cannot due to lack of cryptographic security<sup>6</sup>. Hence, upon a reboot, Crystalor does *not* require verifying the AE leaf node for protection because it will be verified before it is actually used. In other words, the leaf node AE verification can be omitted at the time of recovery, and the verification is completed lazily and concurrently during nominal operation after the recovery. Thus, Crystalor does not have to read the leaf node data nor compute AE for the leaf node at the reboot time. This yields a significant reduction in the recovery cost (as evaluated in Section 4.3) compared to the non-lazy recovery of SCUE because the leaf node occupies a major part of encrypted memory. Such a lazy strategy was adopted in some previous studies [88], and is covered by the provable security of ELM/PAT. An attacker in a practical use scenario of memory encryption, who can manipulate off-chip data and trigger crashes, cannot bypass the recovery tag verification and PAT verification simultaneously, while their combination thereof detects any replay.

## 4 PERFORMANCE EVALUATION

### 4.1 Algorithm-level evaluation

We consider a typical SC parameter [33, 60]: the lengths of major and minor counters (*i.e.*,  $I_{Ma}$  and  $I_{mi}$ ) are 56 and 8 bits, respectively, and the number of nodes sharing a major counter (*i.e.*,  $k$ ) is 8.

SC was originally proposed as an optimization method to reduce the metadata size (*i.e.*, memory overhead). The reduction of metadata size also contributes to a latency reduction because the length of data to be verified by MAC and the amount of communication between memory and CPU are reduced. We derive the relation between the covered region size and ELM parameters to calculate the (optimal) latency of ELM for a given covered region size. Subsequently, we can select an optimal parameter that covers the region with the minimum latency. Note here that the advantages of SC directly represent the supremacy of Crystalor over SCUE.

**Latency and covered region size.** Let  $b$  denote the number of input blocks to MAC and let  $\ell$  denote the bit length of a leaf node. Here,  $b$  is derived from the tree arity  $\beta$  as  $b = \beta/2$  and  $b = \beta/8$  without and with SC, respectively. Without SC, an intermediate node has  $2b$  child nodes because a counter is represented by 64 bits. This indicates that the tree has  $2^d b^d$  leaf nodes. If SC is applied, an intermediate node can have  $8b$  nodes because an input block  $D[i]$  consists of a 64-bit major counter and 8-bit minor counters of

<sup>6</sup>Upon a crash, an attacker can insert a replay data without SCUE detected by incrementing another leaf node counter, such that the sum of leaf node counters is preserved. If the replayed node is loaded before detecting the incremented counters, the replay attack is not detected and succeeds. Thus, entire leaf node AE verification is mandatory to detect such a replay with a counter increment. This implies the insecurity of lazy recovery for SCUE. Thus, SCUE essentially requires verifying the leaf node AE at the timing of recovery.

**Table 1: Latency and covered region of ELM with and without SC, where  $b$  is number of input blocks (corresponding to tree arity),  $\ell$  is bit length of AE, and  $d$  is tree depth**

$b$	$\ell$	Update <sup>†</sup>	Verify	Covered region [Byte]					
				ELM w/o SC			ELM with SC		
				$d = 3$	$d = 5$	$d = 7$	$d = 3$	$d = 5$	$d = 7$
4	512	21	18	33 K	2 M	134 M	2 M	2 G	2 T
	1,024	25	22	66 K	4 M	268 M	4 M	4 G	4 T
	2,048	33	30	131 K	8 M	537 M	8 M	8 G	9 T
	4,096	49	46	262 K	17 M	1 G	17 M	17 G	18 T
	8,192	81	78	524 K	34 M	2 G	34 M	34 G	35 T
8	512	22	20	262 K	67 M	17 G	17 M	69 G	281 T
	1,024	25	22	524 K	134 M	34 G	34 M	137 G	563 T
	2,048	33	30	1 M	268 M	69 G	67 M	275 G	1 P
	4,096	49	46	2 M	537 M	137 G	134 M	550 G	2 P
	8,192	81	78	4 M	1 G	274 G	268 M	1 T	5 P
16	512	30	28	2 M	2 G	2 T	134 M	2 T	36 P
	1,024	30	28	4 M	4 G	4 T	268 M	4 T	72 P
	2,048	33	30	8 M	9 G	9 T	537 M	9 T	144 P
	4,096	49	46	17 M	17 G	18 T	1 G	18 T	288 P
	8,192	81	78	34 M	34 G	35 T	2 G	35 T	576 P
32	512	46	44	17 M	69 G	281 T	1 G	70 T	5 E
	1,024	46	44	34 M	137 G	563 T	2 G	141 T	9 E
	2,048	46	44	67 M	275 G	1 P	4 G	281 T	18 E
	4,096	49	46	134 M	550 G	2 P	9 G	563 T	37 E
	8,192	81	78	268 M	1 T	5 P	17 G	1 P	74 E
64	512	78	76	134 M	2 T	36 P	9 G	2 P	590 E
	1,024	78	76	268 M	4 T	72 P	17 G	5 P	1 Z
	2,048	78	76	537 M	9 T	144 P	34 G	9 P	2 Z
	4,096	78	76	1 G	18 T	288 P	69 G	18 P	5 Z
	8,192	81	78	2 G	35 T	576 P	137 G	36 P	9 Z
128	512	142	140	1 G	70 T	5 E	69 G	72 P	76 Z
	1,024	142	140	2 G	141 T	9 E	137 G	144 P	151 Z
	2,048	142	140	4 G	281 T	18 E	275 K	288 P	302 Z
	4,096	142	140	9 G	563 T	37 E	550 K	576 P	604 Z
	8,192	142	140	17 G	1 P	74 E	1 P	1 Z	1 Y

<sup>†</sup> "Update" actually means "Verify then Update," because PAT requires tag verification always before update for security [15, 34].

eight child nodes. This indicates that the tree with SC has  $2^{3d} b^d$  leaf nodes. For given  $b$  and  $\ell$ , ELM can cover a region of  $2^d b^d \ell$  and  $2^{3d} b^d \ell$  bits without and with SC, respectively. Meanwhile, the update latencies of Flat-OCB and PXOR-MAC hardware in [34] are  $14 + \ell/128$  and  $12 + b$  clock cycles, respectively. Note that the metadata size does not include bits to indicate the address because it is implicit. Table 1 reports the latency and covered region size for different values of  $b$  and  $\ell$  without and with SC, where the latency means  $\min(14 + \lceil \ell/128 \rceil, 12 + b)$  as the bottleneck. From Table 1, we confirm that SC significantly reduces the latency to cover a given region. For example, for  $d = 5$  and 7, to cover a 4 TB region, ELM without SC requires at least 78 and 30 clock cycles for the update, whereas ELM with SC requires only 30 and 22 clock cycles, respectively. Thus, SC reduces the latency overhead by 38 and 8 cycles for  $d = 5$  and 7 (*i.e.*, 62% and 29%), respectively.

**Metadata size.** We evaluate the contribution of SC to reducing the memory overhead for storing metadata. Without SC, the metadata size is  $112 \sum_{i=0}^d \beta^i - 56$ , whereas with SC, it is  $72 \sum_{i=0}^d \beta^i - 56 \sum_{i=0}^{d-1} \beta^i$ , according to [33]. For example, to cover a 4 TB region with a tree of  $b = 4$ , ELM without and with SC has an overhead of 554 GB and 312 GB for storing the metadata, respectively, which indicates a 44% reduction of the overhead by SC. Thus, SC significantly improves the memory encryption performance.

**Additional latency due to minor counter overflow.** When a major counter is incremented (*i.e.*, a minor counter overflows), SC requires the re-computation of tags related to the major counter. If the  $j$ -th node of  $i$ -th major counter overflows, then the major

counter  $\text{ctr}_{\text{Ma}}[i]$  is incremented, and the minor counters  $\text{ctr}_{\text{mi}}[i][j]$  for all  $j$  ( $1 \leq j \leq k$ ) are reset to zero. We should recompute the tag of nodes for all  $j$ , as its nonce counter  $\text{ctr}_{\text{Ma}}[i] \parallel \text{ctr}_{\text{mi}}[i][j]$  is updated. This means that  $k - 1$  MAC/AE updates accompany a minor counter overflow. The system-level simulation for the performance evaluation should regard the latency due to minor counter overflow. Nevertheless, the latency overhead by minor counter overflow is not critical as its frequency is low. On average, it incurs less than one clock cycle latency per store operation.

*Remark 4.1* (Tree depth and hardware resource). The tree depth  $d$  is a parameter that exploits tradeoffs between a *hardware resource* (*i.e.*, the number of MAC engines) and covered region/latency, while  $b$  and  $\ell$  optimal in terms of latency are determined systematically for a given covered region. In other words, for an optimal fixed  $b$  and  $\ell$ , we can enlarge the covered region size by increasing  $d$ , using  $d - 1$  parallel MAC engines. Conversely, we can reduce the latency for a fixed covered size by increasing  $d$ . Thus, the significance of covered region size and improvement by SC depend on  $d$ .

## 4.2 System-level simulation

We performed system-level simulations using the gem5 simulator [10] for the validation. Here, we simulated a CPU with an encrypted main memory (NVM) as same as previous studies, while it is applicable to standard DRAM as well. In this simulation, we evaluated the memory encryption mechanisms with ELM, which is the state-of-the-art and achieves the highest performance among PATs<sup>7</sup>. We assumed to utilize AE and MAC hardware presented in [34] for the ELM hardware in this evaluation. We evaluated the proposed and existing methods as follows:

- Insecure: Memory without any security mechanism.
- ELM w/o SC: ELM not using SC (not recoverable).
- ELM with SC: ELM using SC (not recoverable).
- ELM-SCUE: ELM with SCUE [32] (SC is inapplicable).
- ELM-ASIT: ELM with Anubis [88] (SC is inapplicable).
- ELM-Crystalor (this work): ELM with Crystalor, to which SC is applied.

Insecure and ELMs (not recoverable) were the baselines to evaluate the overhead of PAT and crash recoverability, respectively. We determined the latency according to the memory capacity (*i.e.*, 4 TB) and Table 1. For the ease, feasibility, and reproducibility of the experiment, we employed several simplifications for the simulation and previous studies. We omitted the simulation of packet metadata written to memory. We virtually inserted the latency to write and store operations owing to ELM according to Table 1. For ELM with SC, to evaluate the latency about minor counter overflow, we employed an apportionment, in which we assumed that the writings to memory were uniformly distributed, calculated the expected latency due to the minor counter overflow, and added the

<sup>7</sup>Some previous studies (*e.g.*, [32]) utilized a classical HMAC, which is assumed to require 40, 80, or 160 clock cycles for Verify and Update. However, its concrete realization/implementation was not mentioned, and the number of input blocks to AE/MAC, which actually determines the latency, was not considered. Thus, its practical validity is unclear. We employ the ELM-style evaluation to determine the clock cycles for a fair, modern, and practical performance comparison. Our results are based on the in-depth evaluation of latency in the ELM paper, which considers a concrete cryptographic hardware implementation and the number of input blocks to AE/MAC, while previous studies did not. Note that HMAC is not optimal in terms of latency and is not incremental, while PXOR-MAC in ELM was proposed for an optimized latency [34].

**Table 2: Simulation conditions**

CPU and caches	
CPU core	One core, out-of-order, 2.4 GHz
L1 instruction cache	32 KB, 8-way, 2 cycles
L1 data cache	64 KB, 8-way, 2 cycles
L2 cache	32 KB, 8-way, 2 cycles
Metadata cache	256 kB with cache line 64 byte
Memory controller and main memory (NVM)	
WPQ size	8 entries
Memory latency	Read 50 ns and Write 150 ns
Memory size (covered region)	4 TB
ELM ( $d = 5$ ), to which SC is applied	
Update and verify latency	30 and 28 cycles
Tree parameters	$b = 16$ and $\ell = 1,024$
ELM ( $d = 5$ ), to which SC is inapplicable/not applied	
Update and verify latency	78 and 76 cycles
Tree parameters	$b = 64$ and $\ell = 1,024$
ELM ( $d = 7$ ), to which SC is applied	
Update and verify latency	22 and 20 cycles
Tree parameters	$b = 8$ and $\ell = 1,024$
ELM ( $d = 7$ ), to which SC is inapplicable/not applied	
Update and verify latency	30 and 28 cycles
Tree parameters	$b = 16$ and $\ell = 1,024$

rounded-up value to the latency in Table 1. These simplifications were applied to all of the above methods, which enabled a fair and sound comparison in addition to reproducibility.

We employed a benchmarking workload set, which has been commonly used in many previous studies as a de facto standard (*e.g.*, [31, 43, 81, 90]). The workloads include random insertions of data to a hash table (HT), binary search tree (BST), red-black tree (RBT), and queue (Queue), each of which has a distinct memory access pattern. To analyze the difference, we simulated the workloads with data sizes of 64, 512, 1,024, and 4,096 bytes.

**Results.** Figure 8 reports the normalized workload execution times of the gem5 simulation, in which Insecure is the baseline. We did not evaluate  $d = 3$ , as ELM with  $d = 3$  without SC cannot cover a 4 TB region with a practical latency (this demonstrates the significance of SC). ELM-Crystalor exhibits almost the same performance as ELM with SC. As well, ELM-SCUE and ELM without SC are the almost same. As Crystalor and SCUE incur no latency overhead under nominal operation, the performances of ELM-Crystalor and ELM-SCUE depend solely on the tree parameter. In contrast, ASIT incurs a non-trivial latency overhead to verify and update the shadow table. Comparing ELM with and without SC (*i.e.*, ELM-Crystalor and ELM-SCUE), the performance gain by SC is more significant when the data size is larger. This is because the reduction in latency in reading and storing (*i.e.*, verifying and updating) memory data is more dominant and visible as the numbers of data read and write increase for a larger data size. In addition, the improvement in execution time by SC is more significant when  $d = 5$  than  $d = 7$ , because the reduction ratio of latency by SC is larger when  $d = 5$  for covering a 4 TB region. Thus, we confirm that ELM-Crystalor can reduce the workload execution time by at most 11.5% compared to the state-of-the-art mechanism (*i.e.*, ELM-SCUE).

**Improved scalability for larger memory.** Regarding the tree depth  $d$ , the performance gain by the proposed method is greater for a shallower tree (*i.e.*,  $d = 5$  in this experiment). Recall that  $d$  is a parameter that exploits tradeoffs between a hardware resource (*i.e.*, the number of MAC engines) and a covered region. As the

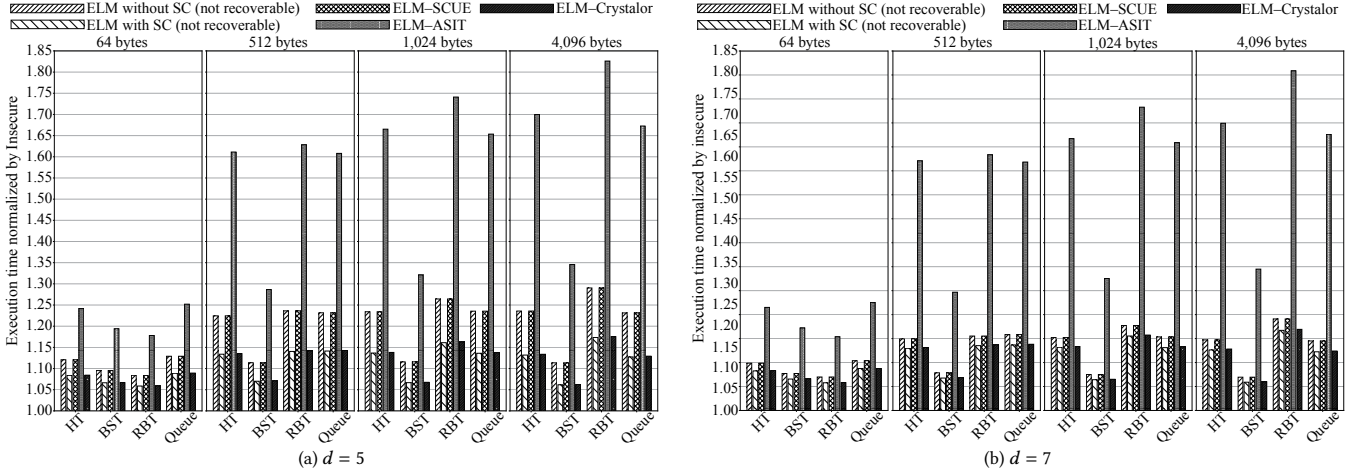


Figure 8: Simulated execution times normalized by Insecure, where proposed method is right-most bin for each workload.

cover region size in the experiment is fixed at 4 TB, the size is relatively larger for  $d = 5$ , and the latency overhead by PAT-based protection is larger for  $d = 5$ . The SC compresses the tree/metadata size more effectively when protecting a larger memory. Hence, the performance gain by SC (and the proposed method) is greater for  $d = 5$ . More quantitatively, for a given arity  $\beta$ , the use of SC can reduce the number of input blocks to PXOR-MAC to  $1/4$  in the used parameter. This indicates that the use of SC reduces the latency of PXOR-MAC asymptotically by  $1/4$  for a larger  $\beta$ . Thus, the use of SC (and ELM-Crystalor) reduces the latency of the memory read/write by up to  $1/4$  when protecting a larger memory. The experimental results on  $d = 5$  and  $7$  indicate an improved scalability.

### 4.3 Recovery cost estimation

**Lazy recovery cost of Crystalor.** We consider here an ELM-Crystalor with SC, whose major and minor counters are 56 and 8 bits, respectively. The recovery time of Crystalor is evaluated by the number of AES calls for PXOR-Hash of recovery tag verification and PXOR-MAC of a new tree construction. To protect an  $M$ -bit memory, the number of AES calls in PXOR-Hash is equivalent to  $M/8\ell$ , while the leaf node verification by Flat-OCB is not required at the time of recovery as mentioned in Section 3.5. In addition, for arity of  $\beta$ , a PXOR-MAC computation requires  $1 + \beta/8$  AES calls, while a new tree construction is realized with  $\sum_{i=1}^d \beta^{i-1}$  PXOR-MAC computations. This indicates that the new tree construction requires  $(1 + \beta/8) \sum_{i=1}^d \beta^{i-1}$  AES calls in total. Moreover, a new tree construction requires computations of new counter value  $\sum_{i=1}^d \beta^{i-1}$  times. Recall that  $M = \beta^d \ell$ . Thus, Crystalor recovery is realized with  $\beta^d/8 + (1 + \beta/8) \sum_{i=1}^d \beta^{i-1}$  AES calls and  $\sum_{i=1}^d \beta^{i-1}$  new counter computations, which corresponds to the number of intermediate nodes (including root node). In addition, Crystalor requires to read  $8\beta^d$  bits of leaf node metadata from memory, while Crystalor writes  $16(4 + \beta) \sum_{i=2}^d \beta^{i-1}$  bits of metadata to memory during a recovery. Owing to the lazy recovery, the costs are independent of the leaf node bit length (*i.e.*,  $\ell$ ).

**Recovery cost of SCUE.** For comparison, we consider ELM-SCUE recovery with a 64-bit counter. Its recovery cost is evaluated by the number of counter-summings and PXOR-MAC computations. The equivalence check between the root counter and the sum of leaf node counters requires  $\sum_{i=1}^d \beta^{i-1}$  counter-summings. The tree recovery performs one counter-summings and one PXOR-MAC computation per node. A PXOR-MAC requires  $1 + \beta/2$  AES calls and  $\sum_{i=1}^d \beta^{i-1}$  intermediate nodes exist. The leaf node AE verification requires  $\beta^d (\lceil \ell/128 \rceil + 1)$  AES calls. Thus, the computational cost is  $2 \sum_{i=1}^d \beta^{i-1}$  counter-summings and  $\beta^d (\lceil \ell/128 \rceil + 1) + (1 + \beta/2) \sum_{i=1}^d \beta^{i-1}$  AES calls. Meanwhile, SCUE reads  $\beta^d \ell + 64\beta^d$  bits from memory and it writes  $64(1 + \beta) \sum_{i=2}^d \beta^{i-1}$  bits to memory.

**Evaluation result.** Figure 9a and Figure 9b report the computational cost (*i.e.*, the number of clock cycles) and the communication cost between CPU and memory for some covered region sizes, respectively. Here, the throughputs of the counter-summings, new counter computation, and one block AES encryption are assumed to be one per clock cycle [15, 34]. In Figure 9b, we evaluated by the number of transmitted bits, in which the writing cost was tripled as in Table 2. Crystalor achieved a reduction of 90–99.9% of recovery costs from SCUE, owing to the lazy recovery. Although the computational and traffic costs of the leaf node AE verification is a major part of SCUE (*i.e.*,  $\beta^d (\lceil \ell/128 \rceil + 1)$  AES calls and  $\beta^d \ell$  bits read, respectively), Crystalor does not require them. Thus, we confirm the advantage of Crystalor in recovery cost as well as the performance.

## 5 CONCLUSION

This study presented Crystalor, an L4-secure memory encryption mechanism. Crystalor incurs almost no latency overhead under nominal operation and achieves an efficient recovery. Although existing mechanisms (*e.g.*, SCUE) are incompatible with structural optimizations, Crystalor fully exploits its advantages and offers the same security and recoverability. We algorithmically and experimentally confirmed that Crystalor has a significant advantage over conventional mechanisms in terms of the memory overhead and execution time/latency, with a reduced recovery cost. At the

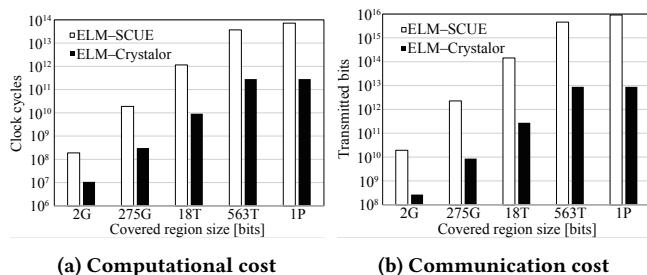


Figure 9: Estimation of recovery costs.

algorithmic level, for protecting a 4 TB memory with ELM, Crystalor requires 29–62% fewer clock cycles per memory read/write operation than SCUE, while Crystalor and SCUE require 312 GB and 554 GB memory overheads for storing metadata, respectively (namely, Crystalor achieves a 44% reduction of memory overhead). We performed a system-level simulation using the gem5 simulator. We confirmed that Crystalor achieves a reduction in the workload execution time by at most 11.5% from SCUE. Moreover, Crystalor offers a lazy recovery owing to its cryptographic protection, which achieved a recovery that is several thousands faster than SCUE.

We employed the SC as the most typical optimization technique for PAT. Alternatively, Crystalor can work with any structural optimization as it employs cryptographic protection. Its evaluation with other optimization techniques are important future work.

## REFERENCES

- [1] 2023. AMD Secure Encrypted Virtualization (SEV). <https://www.amd.com/en/developer/sev.html>. (2023). Visited in September 2023.
- [2] 2023. Intel Optane Technology. <https://www.intel.com/content/www/us/en/architecture-and-technology/optane-technology/optane-for-data-centers.html>. (2023). Visited in September 2023.
- [3] Mazen Alwadi, Kazi Abu Zubair, David Mohaisen, and Amro Awad. 2020. Phoenix: Towards Ultra-Low Overhead, Recoverable, and Persistently Secure NVM. *IEEE Transactions on Dependable and Secure Computing* 19, 2 (2020), 1049–1063.
- [4] Roberto Avanzi. 2017. The QARMA Block Cipher Family. Almost MDS Matrices Over Rings With Zero Divisors, Nearly Symmetric Even-Mansour Constructions With Non-Involutory Central Rounds, and Search Heuristics for Low-Latency S-Boxes. *IACR Trans. Symmetric Cryptol.* 2017, 1 (2017), 4–44.
- [5] Roberto Avanzi, Subhadeep Banik, Orr Dunkelman, Hector Montaner, Prakash Ramrakhiani, Francesco Regazzoni, and Andreas Sandberg. 2020. Protecting Memory Contents on ARM Cores. *Real World Crypto (RWC)*. (2020). <https://rwc.iacr.org/2020/slides/Avanzi.pdf>
- [6] Roberto Avanzi, Andreas Sandberg, Ionut Mihalcea, David Schall, and Héctor Montaner. 2022. SoK: Hardware-Supported Cryptographic Protection of Random Access Memory. *Cryptology ePrint Archive, Paper 2022/1472*. (2022). <https://eprint.iacr.org/2022/1472> <https://eprint.iacr.org/2022/1472>.
- [7] Amro Awad, Mao Ye, Yan Solihin, Laurent Njilla, and Kazi Abu Zubair. 2019. Triad-NVM: Persistency for Integrity-Protected and Encrypted Non-Volatile Memories. In *ACM/IEEE 46th Annual International Symposium on Computer Architecture (ISCA '19)*. 104–115.
- [8] Mihir Bellare, Oded Goldreich, and Shafi Goldwasser. 1995. Incremental Cryptography and Application to Virus Protection. In *Proceedings of the Twenty-Seventh Annual ACM Symposium on Theory of Computing (STOC '95)*. Association for Computing Machinery, New York, NY, USA, 454–456. <https://doi.org/10.1145/225058.225080>
- [9] Mihir Bellare and Chanathip Namprempre. 2008. Authenticated Encryption: Relations among Notions and Analysis of the Generic Composition Paradigm. *Journal of Cryptology* 21 (2008), 469–491.
- [10] Nathan Binkert, Bradford Beckmann, Gabriel Black, Steven K. Reinhardt, Ali Saidi, Arkaprava Basu, Joel Hestness, Derek R. Hower, Tushar Krishna, Somayeh Sardashti, Rathijit Sen, Korey Sewell, Muhammad Shoaib, Nilay Vaish, Mark D. Hill, and David A. Wood. 2011. The Gem5 Simulator. *SIGARCH Comput. Archit. News* 39, 2 (Aug. 2011), 1–7. <https://doi.org/10.1145/2024716.2024718> Place: New York, NY, USA Publisher: Association for Computing Machinery.
- [11] Julia Borghoff, Anne Canteaut, Tim Güneysu, Elif Bilge Kavun, Miroslav Knezevic, Lars R. Knudsen, Gregor Leander, Ventsislav Nikov, Christof Paar, Christian Rechberger, Peter Rombouts, Søren S. Thomsen, and Tolga Yalçın. 2012. PRINCE - A Low-Latency Block Cipher for Pervasive Computing Applications - Extended Abstract. In *ASIACRYPT (Lecture Notes in Computer Science)*, Vol. 7658. Springer, 208–225.
- [12] Robert Buhren, Hans-Niklas Jacob, Thilo Krachenfels, and Jean-Pierre Seifert. 2021. One Glitch to Rule Them All: Fault Injection Attacks Against AMD’s Secure Encrypted Virtualization. In *ACM SIGSAC Conference on Computer and Communications Security (CCS)*. Association for Computing Machinery, New York, NY, USA, 2875–2889. <https://doi.org/10.1145/3460120.3484779>
- [13] Federico Canale, Tim Güneysu, Gregor Leander, Jan Thoma, Yosuke Todo, and Rei Ueno. 2023. SCARF: A Low-Latency Block Cipher for Secure Cache-Randomization. In *32nd USENIX Security Symposium*. <https://eprint.iacr.org/2022/1228>
- [14] J. Lawrence Carter and Mark N. Wegman. 1979. Universal classes of hash functions. *J. Comput. System Sci.* 18, 2 (1979), 143–0154. [https://doi.org/10.1016/0022-0000\(79\)90044-8](https://doi.org/10.1016/0022-0000(79)90044-8)
- [15] Victor Costan and Srinivas Devadas. 2016. Intel SGX explained. *Cryptology ePrint Archive, Paper 2016/086*. (2016). <https://eprint.iacr.org/2016/086>
- [16] Nai-Jia Dong, Hsiang-Yun Cheng, Chia-Lin Yang, Bo-Rong Lin, and Hsiang-Pang Li. 2022. Efficient and Atomic-Durable Persistent Memory through In-PM Hybrid Logging. In *2022 IEEE 11th Non-Volatile Memory Systems and Applications Symposium (NVMSA)*. 1–7. <https://doi.org/10.1109/NVMSA56066.2022.00010>
- [17] Morris J. Dworkin. 2001. *SP 800-38A 2001 edition. Recommendation for block cipher modes of operation: Methods and techniques*. Technical Report. National Institute of Standards & Technology, Gaithersburg, MD, USA.
- [18] Morris J. Dworkin. 2005. *SP 800-38B. Recommendation for Block Cipher Modes of Operation: The MAC Mode for Authentication*. Technical Report. Gaithersburg, MD, USA.
- [19] Tetsuo Endoh, Hiroaki Honjo, Koichi Nishioka, and Shoji Ikeda. 2020. Recent Progresses in STT-MRAM and SOT-MRAM for Next Generation MRAM. In *2020 IEEE Symposium on VLSI Technology*. 1–2. <https://doi.org/10.1109/VLSITechnology18217.2020.9265042>
- [20] Ali Fakhrazadehgan, Yale N. Patt, Prashant J. Nair, and Moinuddin K. Qureshi. 2022. SafeGuard: Reducing the Security Risk from Row-Hammer via Low-Cost Integrity Protection. In *2022 IEEE International Symposium on High-Performance Computer Architecture (HPCA)*. 373–386. <https://doi.org/10.1109/HPCA53966.2022.00035>
- [21] Alexander Freij, Huiyang Zhou, and Yan Solihin. 2021. Bonsai Merkle Forests: Efficiently Achieving Crash Consistency in Secure Persistent Memory. In *54th Annual IEEE/ACM International Symposium on Microarchitecture*. 1227–1240.
- [22] Blaise Gassend, G. Edward Suh, Dwaine Clarke, Marten van Dijk, and Srinivas Devadas. 2003. Caches and Hash Trees for Efficient Memory Integrity Verification. In *the 9th International Symposium on High-Performance Computing Architecture*.
- [23] Peter Gazi, Krzysztof Pietrzak, and Michal Rybár. 2016. The Exact Security of PMAC. *IACR Trans. Symmetric Cryptol.* 2016, 2 (2016), 145–161.
- [24] Hannes Gross, Stefan Mangard, and Thomas Korak. 2016. Domain-Oriented Masking: Compact Masked Hardware Implementations with Arbitrary Protection Order. In *ACM Workshop on Theory of Implementation Security (TIS 2016)*. 3.
- [25] Shay Gueron. 2016. A Memory Encryption Engine Suitable for General Purpose Processors. *Cryptology ePrint Archive, Paper 2016/204*. (2016). <https://eprint.iacr.org/2016/204> <https://eprint.iacr.org/2016/204>.
- [26] Shay Gueron. 2016. Memory Encryption for General-Purpose Processors. *IEEE Secur. Priv.* 14, 6 (2016), 54–62.
- [27] Richard H. Gumpertz. 1983. Combining tags with error codes. In *10th Annual International Symposium on Computer Architecture (ISCA)*. 160–165.
- [28] J. Alex Halderman, Seth D. Schoen, Nadia Heninger, William Clarkson, William Parl, Joseph A. Calandrino, Ariel J. Feldman, Jacob Appelbaum, and Edward W. Felten. 2009. Lest we remember: cold-boot attacks on encryption keys. *Communication of the ACM* 52 (2009), 91–98. Issue 5.
- [29] W. Eric Hall and Charanjit S. Jutla. 2006. Parallelizable Authentication Trees. In *Selected Areas in Cryptography*. Springer Berlin Heidelberg, 95–109.
- [30] Xijiang Han, James Tuck, and Arno Awad. 2021. Dolos: Improving the Performance of Persistent Applications in ADR-Supported Secure Memory. In *54th Annual IEEE/ACM International Symposium on Microarchitecture (MICRO)*. 1241–1253.
- [31] Jianming Huang and Yu Hua. 2021. A Write-Friendly and Fast-Recovery Scheme for Security Metadata in Non-Volatile Memories. In *2021 IEEE International Symposium on High-Performance Computer Architecture (HPCA)*. IEEE, Seoul, Korea (South), 359–370. <https://doi.org/10.1109/HPCA51647.2021.00038>
- [32] Jianming Huang and Yu Hua. 2023. Root crash consistency of SGX-style integrity trees in secure non-volatile memory systems. In *Proceedings of the 29th IEEE International Symposium on High-Performance Computer Architecture*

- (HPCA).
- [33] Akiko Inoue, Kazuhiko Minematsu, Maya Oda, Rei Ueno, and Naofumi Homma. 2020. ELM: A Low-Latency and Scalable Memory Encryption Scheme. Cryptology ePrint Archive, Paper 2020/1374. (2020). <https://eprint.iacr.org/2020/1374> Preliminary and long version of a paper with same title.
  - [34] Akiko Inoue, Kazuhiko Minematsu, Maya Oda, Rei Ueno, and Naofumi Homma. 2022. ELM: A Low-Latency and Scalable Memory Encryption Scheme. *IEEE Transactions on Information Forensics and Security* 17 (2022), 2628–2643. <https://doi.org/10.1109/TIFS.2022.3188146>
  - [35] Jungi Jeong, Chang Hyun Park, Jaehyuk Huh, and Seungryoul Maeng. 2018. Efficient Hardware-Assisted Logging with Asynchronous and Direct-Update for Persistent Memory. In *2018 51st Annual IEEE/ACM International Symposium on Microarchitecture (MICRO)*. 520–532. <https://doi.org/10.1109/MICRO.2018.00049>
  - [36] Arpit Joshi, Vijay Nagarajan, Stratis Viglas, and Marcelo Cintra. 2017. ATOM: Atomic Durability in Non-volatile Memory through Hardware Logging. In *2017 IEEE International Symposium on High Performance Computer Architecture (HPCA)*. 361–372. <https://doi.org/10.1109/HPCA.2017.50>
  - [37] Yoongu Kim, Ross Daly, Jeremie Kim, Chris Fallin, Ji Hye Lee, Donghyuk Lee, Chris Wilkerson, Konrad Lai, and Onur Mutlu. 2014. Flipping bits in memory without accessing them: An experimental study of DRAM disturbance errors. In *2014 ACM/IEEE 41st International Symposium on Computer Architecture (ISCA)*. 361–372. <https://doi.org/10.1109/ISCA.2014.6853210>
  - [38] Paul Kocher, Jann Horn, Anders Fogh, Daniel Genkin, Daniel Gruss, Werner Haas, Mike Hamburg, Moritz Lipp, Stefan Mangard, Thomas Prescher, Michael Schwarz, and Yuval Yarom. 2019. Spectre Attacks: Exploiting Speculative Execution. In *2019 IEEE Symposium on Security and Privacy (S&P)*. 1–19. <https://doi.org/10.1109/SP.2019.00002>
  - [39] Paul Kocher, Joshua Jaffe, and Benjamin Jun. 1999. Differential Power Analysis. In *Advances in Cryptology—CRYPTO 1999 (Lecture Notes in Computer Science)*, Vol. 1666. Springer, 388–397.
  - [40] Paul C. Kocher. 1996. Timing Attacks on Implementations of Diffie-Hellman, RSA, DSS, and Other Systems. In *Advances in Cryptology—CRYPTO 1996 (Lecture Notes in Computer Science)*, Vol. 1109. Springer, 104–113.
  - [41] Andrew Kwong, Daniel Genkin, Daniel Gruss, and Yuval Yarom. 2020. RAM-Bleed: Reading Bits in Memory Without Accessing Them. In *2020 IEEE Symposium on Security and Privacy (SP)*. 695–711. <https://doi.org/10.1109/SP40000.2020.00020>
  - [42] Lamster, Martin Unterguggenberger, David Schrammel, and Stefan Mangard. 2023. HashTag: Hash-Based Integrity Protection for Tagged Architectures. In *32nd USENIX Security Symposium (USENIX Security 23)*. USENIX Association, Anaheim, CA, 2797–2814. <https://www.usenix.org/conference/usenixsecurity23/presentation/lamster>
  - [43] Mengya Lei, Fan Li, Fang Wang, Dan Feng, Xiaomin Zou, and Renzhi Xiao. 2022. SecNVM: An Efficient and Write-Friendly Metadata Crash Consistency Scheme for Secure NVM. *ACM Transactions on Architecture and Code Optimization* 19, 1 (March 2022), 1–26. <https://doi.org/10.1145/3488724>
  - [44] Mengyuan Li, Luca Wilke, Jan Wichelmann, Thomas Eisenbarth, Radu Teodorescu, and Yinqian Zhang. 2022. A Systematic Look at Ciphertext Side Channels on AMD SEV-SNP. In *2022 IEEE Symposium on Security and Privacy (SP)*. 337–351. <https://doi.org/10.1109/SP46214.2022.9833768>
  - [45] Mengyuan Li, Yinqian Zhang, Zhiqiang Lin, and Yan Solihin. 2019. Exploiting Unprotected I/O Operations in AMD’s Secure Encrypted Virtualization. In *28th USENIX Security Symposium (USENIX Security 19)*. USENIX Association, Santa Clara, CA, 1257–1272. <https://www.usenix.org/conference/usenixsecurity19/presentation/li-mengyuan>
  - [46] Mengyuan Li, Yinqian Zhang, HuiBo Wang, Kang Li, and Yueqiang Cheng. 2021. CIPHERLEAKS: Breaking Constant-time Cryptography on AMD SEV via the Ciphertext Side Channel. In *30th USENIX Security Symposium (USENIX Security 21)*. USENIX Association, 717–732. <https://www.usenix.org/conference/usenixsecurity21/presentation/li-mengyuan>
  - [47] Moritz Lipp, Michael Schwarz, Daniel Gruss, Thomas Prescher, Werner Haas, Anders Fogh, Jann Horn, Stefan Mangard, Paul Kocher, Daniel Genkin, Yuval Yarom, and Mike Hamburg. 2018. Meltdown: Reading Kernel Memory from User Space. In *27th USENIX Security Symposium (USENIX Security 18)*. USENIX Association, Baltimore, MD, 973–990. <https://www.usenix.org/conference/usenixsecurity18/presentation/lipp>
  - [48] Fangfei Liu, Yuval Yarom, Qian Ge, Gernot Heiser, and Ruby B Lee. 2015. Last-Level Cache Side-Channel Attacks are Practical. In *IEEE Symposium on Security and Privacy*. IEEE, 244–256.
  - [49] Sihang Liu, Aasheesh Kolli, Jinglei Ren, and Samira Khan. 2018. Crash Consistency in Encrypted Non-volatile Main Memory Systems. In *2018 IEEE International Symposium on High Performance Computer Architecture (HPCA)*. 310–323. <https://doi.org/10.1109/HPCA.2018.00035> ISSN: 2378-203X.
  - [50] Sihang Liu, Aasheesh Kolli, Jinglei Ren, and Samira Khan. 2018. Crash Consistency in Encrypted Non-volatile Main Memory Systems. In *2018 IEEE International Symposium on High Performance Computer Architecture (HPCA)*. 310–323. <https://doi.org/10.1109/HPCA.2018.00035>
  - [51] Stefan Mangard, Elisabeth Oswald, and Thomas Popp. 2007. *Power Analysis Attacks: Revealing the Secrets of Smart Cards*. Springer New York.
  - [52] Ralph C. Merkle. 1979. Method of providing digital signatures. US4309569A. (1979). <https://patents.google.com/patent/US4309569>.
  - [53] Ralph C. Merkle. 1988. A Digital Signature Based on a Conventional Encryption Function. In *Advances in Cryptology—CRYPTO ’87*. Springer Berlin Heidelberg, Berlin, Heidelberg, 369–378.
  - [54] Kazuhiko Minematsu and Toshiyasu Matsushima. 2007. New Bounds for PMAC, TMAC, and XCBC. In *International Conference on Fast Software Encryption (FSE) (Lecture Notes in Computer Science)*, Vol. 4593. Springer, 434–451.
  - [55] Ahmad Moghimi, Gorka Irazoqui, and Thomas Eisenbarth. 2017. CacheZoom: How SGX Amplifies the Power of Cache Attacks. In *International Conference on Cryptographic Hardware and Embedded Systems (CHES)*. Springer International Publishing, 69–90.
  - [56] Mathias Morbitzer, Manuel Huber, Julian Horsch, and Sascha Wessel. 2018. SEVered: Subverting AMD’s Virtual Machine Encryption. In *11th European Workshop on Systems Security*. 1–6.
  - [57] Mathias Morbitzer, Sergej Proskurin, Martin Radev, Marko Dorfhuber, and Erick Quintanar Salas. 2021. SEVerity: Code Injection Attacks against Encrypted Virtual Machines. In *2021 IEEE Security and Privacy Workshops (SPW)*. 444–455. <https://doi.org/10.1109/SPW53761.2021.00063>
  - [58] Pascal Nasahl, Robert Schilling, Mario Werner, Jan Hoogerbrugge, Marcel Medwed, and Stefan Mangard. 2021. CrypTag: Thwarting Physical and Logical Memory Vulnerabilities Using Cryptographically Colored Memory. In *Proceedings of the 2021 ACM Asia Conference on Computer and Communications Security (ASIA CCS)*. Association for Computing Machinery, New York, NY, USA, 200aÅ–12. <https://doi.org/10.1145/3433210.3453684>
  - [59] Matheus Almeida Ogleari, Ethan L. Miller, and Jishen Zhao. 2018. Steal but No Force: Efficient Hardware Undo+Redo Logging for Persistent Memory Systems. In *2018 IEEE International Symposium on High Performance Computer Architecture (HPCA)*. 336–349. <https://doi.org/10.1109/HPCA.2018.00037>
  - [60] Qi Pei and Seunghee Shin. 2021. Efficient Split Counter Mode Encryption for NVM. In *2021 IEEE International Symposium on Performance Analysis of Systems and Software (ISPASS)*. 93–95. <https://doi.org/10.1109/ISPASS51385.2021.00026>
  - [61] Qi Pei and Seunghee Shin. 2021. Improving the Heavy Re-encryption Overhead of Split Counter Mode Encryption for NVM. In *2021 IEEE 39th International Conference on Computer Design (ICCD)*. 425–432. <https://doi.org/10.1109/ICCD53106.2021.00073>
  - [62] Antoon Purnal, Lukas Giner, Daniel Gruss, and Ingrid Verbauwhede. 2021. Systematic Analysis of Randomization-based Protected Cache Architectures. In *IEEE Symposium on Security and Privacy (S&P)*. 987–1002.
  - [63] Moinuddin K. Qureshi. 2018. CEASER: Mitigating Conflict-Based Cache Attacks via Encrypted-Address and Remapping. In *51st Annual IEEE/ACM International Symposium on Microarchitecture (MICRO ’51)*. 775–787.
  - [64] Phillip Rogaway. 2002. Authenticated-Encryption with Associated-Data. In *Proceedings of the 9th ACM Conference on Computer and Communications Security (CCS ’02)*. Association for Computing Machinery, New York, NY, USA, 98aÅ–107. <https://doi.org/10.1145/586110.586125>
  - [65] Phillip Rogaway. 2004. Efficient Instantiations of Tweakable Blockciphers and Refinements to Modes OCB and PMAC. In *Advances in Cryptology—ASIACRYPT 2004*. Pil Joong Lee (Ed.), Springer Berlin Heidelberg, Berlin, Heidelberg, 16–31.
  - [66] Phillip Rogaway, Mihir Bellare, and John Black. 2003. OCB: A Block-Cipher Mode of Operation for Efficient Authenticated Encryption. *ACM Trans. Inf. Syst. Secur.* 6, 3 (aug 2003), 365aÅ–403. <https://doi.org/10.1145/937527.937529>
  - [67] Gururaj Saileshwar, Prashant J. Nair, Prakash Ramrakhyan, Wendy Elsasser, Jose A. Joao, and Moinuddin K. Qureshi. 2018. Morphable counters: enabling compact integrity trees for low-overhead secure memories. In *51st Annual IEEE/ACM International Symposium on Microarchitecture*. 416–427.
  - [68] Gururaj Saileshwar, Prashant J. Nair, Prakash Ramrakhyan, Wendy Elsasser, and Moinuddin K. Qureshi. 2018. SYNERGY: Rethinking Secure-Memory Design for Error-Correcting Memories. In *2018 IEEE International Symposium on High Performance Computer Architecture (HPCA)*. 454–465. <https://doi.org/10.1109/HPCA.2018.00046>
  - [69] Seunghee Shin, Satish Kumar Tirukkavalluri, James Tuck, and Yan Solihin. 2017. Proteus: A Flexible and Fast Software Supported Hardware Logging approach for NVM. In *2017 50th Annual IEEE/ACM International Symposium on Microarchitecture (MICRO)*. 178–190.
  - [70] Solid State Storage Initiative. 2014. NVDIMM Messaging and FAQ. (Jan. 2014).
  - [71] Meysam Taassori, Ali Shafiee, and Rajeev Balasubramonian. 2018. VAULT: Reducing Paging Overheads in SGX with Efficient Integrity Verification Structures. In *Proceedings of the Twenty-Third International Conference on Architectural Support for Programming Languages and Operating Systems*. ACM, Williamsburg VA USA, 665–678. <https://doi.org/10.1145/3173162.3177155>
  - [72] Eran Tromer, Dag Arne Osvik, and Adi Shamir. 2010. Efficient Cache Attacks on AES, and Countermeasures. *Journal of Cryptology* 23, 1 (2010), 37–71.
  - [73] Yukiyasu Tsunoo, Teruo Saito, Tomoyasu Suzuki, Maki Shigeri, and Hiroshi Miyachi. 2003. Cryptanalysis of DES Implemented on Computers with Cache.

- In *International Workshop on Cryptographic Hardware and Embedded Systems (CHES 2003)*. Springer Berlin Heidelberg, 62–76.
- [74] Rei Ueno, Sumio Morioka, Noriyuki Miura, Kohei Matsuda, Makoto Nagata, Shivam Bhasin, Yves Mathieu, Tarik Graba, Jean-Luc Danger, and Naofumi Homma. 2020. High Throughput/Gate AES Hardware Architectures Based on Datapath Compression. *IEEE Trans. Comput.* 69, 4 (2020), 534–548. <https://doi.org/10.1109/TC.2019.2957355>
- [75] Thomas Unterluggauer, Mairo Werner, and Stefan Mangard. 2019. MEAS: memory encryption and authentication secure against side-channel attacks. *Journal of Cryptographic Engineering* 9 (2019), 137–158.
- [76] Wubing Wang, Mengyuan Li, Yinqian Zhang, and Zhiqiang Lin. 2023. Pwr-Leak: Exploiting Power Reporting Interface For Side-Channel Attacks AMD SEV. In *International Conference on Detection of Intrusions and Malware, and Vulnerability Assessment (DIMVA)*. Springer-Verlag, Berlin, Heidelberg, 46–66. [https://doi.org/10.1007/978-3-031-35504-2\\_3](https://doi.org/10.1007/978-3-031-35504-2_3)
- [77] Xueliang Wei, Dan Feng, Wei Tong, Jingning Liu, and Liuqing Ye. 2020. Mor-Log: Morphable Hardware Logging for Atomic Persistence in Non-Volatile Main Memory. In *2020 ACM/IEEE 47th Annual International Symposium on Computer Architecture (ISCA)*. 610–623. <https://doi.org/10.1109/ISCA45697.2020.00057>
- [78] Mario Werner, Thomas Unterluggauer, Lukas Giner, Michael Schwarz, Daniel Gruss, and Stefan Mangard. 2019. ScatterCache: Thwarting Cache Attacks via Cache Set Randomization. In *28th USENIX Security Symposium (USENIX Security '19)*. 675–692.
- [79] Luca Wilke, Jan Wichelmann, Mathias Morbitzer, and Thomas Eisenbarth. 2020. SEVurity: No Security Without Integrity : Breaking Integrity-Free Memory Encryption with Minimal Assumptions. In *2020 IEEE Symposium on Security and Privacy (SP)*. 1483–1496. <https://doi.org/10.1109/SP40000.2020.00080>
- [80] Chenyu Yan, D. Engländer, M. Prvulovic, B. Rogers, and Yan Solihin. 2006. Improving Cost, Performance, and Security of Memory Encryption and Authentication. In *33rd International Symposium on Computer Architecture (ISCA'06)*. 179–190. <https://doi.org/10.1109/ISCA.2006.22> ISSN: 1063-6897.
- [81] Fan Yang, Youmin Chen, Haiyu Mao, Youyou Lu, and Jiwu Shu. 2020. Shield-NVM: An Efficient and Fast Recoverable System for Secure Non-Volatile Memory. *ACM Transactions on Storage* 16, 2 (June 2020), 1–31. <https://doi.org/10.1145/3381835>
- [82] Fan Yang, Youyou Lu, Youmin Chen, Haiyu Mao, and Jiwu Shu. 2019. No Compromises: Secure NVM with Crash Consistency, Write-Efficiency and High-Performance. In *56th Annual Design Automation Conference (DAC '19)*. IEEE, 1–6.
- [83] Yuval Yarom and Katrina Falkner. 2014. FLUSH+RELOAD: A High Resolution, Low Noise, L3 Cache Side-Channel Attack. In *23rd USENIX Security Symposium*.
- [84] Chencheng Ye, Yuanhao Xu, Xipeng Shen, Yan Sha, Xiaofei Liao, Hai Jin, and Yan Solihin. 2023. Reconciling Selective Logging and Hardware Persistent Memory Transaction. In *2023 IEEE International Symposium on High-Performance Computer Architecture (HPCA)*. 664–676. <https://doi.org/10.1109/HPCA56546.2023.10071088>
- [85] Mao Ye, Clayton Hughes, and Amro Awad. 2018. Osiris: A Low-Cost Mechanism to Enable Restoration of Secure Non-Volatile Memories. In *2018 51st Annual IEEE/ACM International Symposium on Microarchitecture (MICRO)*. 403–415. <https://doi.org/10.1109/MICRO.2018.00040>
- [86] Zhan Zhang, Jianhui Yue, Xiaofei Liao, and Hai Jin. 2021. Efficient Hardware Redo Logging for Secure Persistent Memory. In *2021 IEEE 23rd Int Conf on High Performance Computing Communications; 7th Int Conf on Data Science Systems; 19th Int Conf on Smart City; 7th Int Conf on Dependability in Sensor, Cloud Big Data Systems Application (HPCC/DSS/SmartCity/DependSys)*. 41–48. <https://doi.org/10.1109/HPCC-DSS-SmartCity-DependSys53884.2021.00033>
- [87] Jian Zhou, Amro Awad, and Jun Wang. 2020. Lelantus: fine-granularity copy-on-write operations for secure non-volatile memories. In *ACM/IEEE 47th Annual International Symposium on Computer Architecture (ISCA '20)*. 597–607.
- [88] Kazi Abu Zubair and Amro Awad. 2019. Anubis: ultra-low overhead and recovery time for secure non-volatile memories. In *Proceedings of the 46th International Symposium on Computer Architecture*. ACM, Phoenix Arizona, 157–168. <https://doi.org/10.1145/3307650.3322252>
- [89] Kazi Abu Zubair, Sudhanva Gurumurthi, Vilas Sridharan, and Amro Awad. 2021. Soteria: Towards Resilient Integrity-Protected and Encrypted Non-Volatile Memories. In *54th Annual IEEE/ACM International Symposium on Microarchitecture*. 1214–1226.
- [90] Pengfei Zuo, Yu Hua, and Yuan Xie. 2019. SuperMem: Enabling Application-transparent Secure Persistent Memory with Low Overheads. In *Proceedings of the 52nd Annual IEEE/ACM International Symposium on Microarchitecture*. ACM, Columbus OH USA, 479–492. <https://doi.org/10.1145/3352460.3358290>